universität wien

MASTERARBEIT / MASTER'S THESIS

Titel der Masterarbeit / Title of the Master's Thesis

"Stability of the ΦCh1 ORF44 deletion mutant and characterization of the function of gp44"

verfasst von / submitted by

Mikaela Andrea Edwards, BSc

angestrebter akademischer Grad / in partial fulfilment of the requirements for the degree of

Master of Science (MSc)

Wien, 2018 / Vienna 2018

Studienkennzahl lt. Studienblatt / degree programme code as it appears on the student record sheet:	A 066 834
Studienrichtung lt. Studienblatt / degree programme as it appears on the student record sheet:	Master Molecular Biology
Betreut von / Supervisor	Ao. Univ.-Prof. Dipl.-Biol. Dr. Angela Witte

Acknowledgements

It is a genuine pleasure to express my sincere gratitude to my supervisor, mentor and guide Ao. Univ.-Prof. Dipl.-Biol. Dr. Angela Witte for the immeasurable support throughout my Master study and research. Having been granted the opportunities to work in her laboratory and work as a tutor for her practical courses has helped me widen my horizon. Her dedication in this scientific field, her hard work and patience are definitely one of the many things I have learnt from her.

In my daily work I have been blessed with a friendly group of laboratory colleagues: I herewith want to thank Jana Dragisic, Matthias Schmal and Richard Manning. I would particularly like to single out Jana for the support, the laughter, and for providing me with something greater than just being a fellow student: her friendship. Likewise, I would like to thank Matthias for showing me around the laboratory and for always helping me find all the necessary equipments and chemicals.

Furthermore, a special note of thanks goes to the members of the neighbouring laboratory Elisabeth Sonnleitner, Petra Pusic and Armin Resch for providing me with helpful advices.

My appreciation also extends to my boyfriend Christopher Soria for patiently joining me in this roller coaster ride of emotions during my research, for listening to all my problems and for encouraging me to keep on going with a smile on my face. Most importantly, I would like to acknowledge my dear parents Elizabeth and Marvin Edwards for their prayers and their guidance, not only throughout my studies, but also throughout this entire journey that brought me to where I am today. “Perseverance is the key to success” – thank you for always reminding me that. And to my one and only sister Cherry Edwards, who has also been remarkably important in the pursuit of my Master’s degree, I am grateful to have such a supportive sister. She is my number one cheerleader, my motivator and my inspiration. My family has always been there for me through thick and thin, through rain and shine.

"Let all the things you do be done in love."

To Daddy, Mommy and Ate Cherry

1. Introduction

1.1. The three domains of life

The classification of biodiversity also evolved drastically over a period of time, wherein the definition of the taxa continuously changed from the organismal up to the molecular level (Woese *et al*., 1990). In the 18th century, it was believed that all living organisms were organized into two specific kingdoms: *Animalia* and *Plantae* (Linnaeus, 1735). In 1866, Haeckel identified unicellular organisms – the so-called *Protista* – which did not fit into both of the two previously classified kingdoms, thus adding a third branch to the tree of life (Haeckel, 1866). A further reestablishment in the classification was achieved by Whittaker in 1969, giving rise to the five-kingdom system: *Animalia, Plantae, Fungi, Protista and Monera* (bacteria) (Whittaker, 1969). This concept co-existed in parallel to that of Edouard Chatton's perception until the late 1970s. Chatton was the first to classify living organisms in *Prokaryotes* and *Eukaryotes* (Sapp, 2005).

In 1977, Woese and Fox came across a universal chronometer enabling investigation of the phylogenetic links. They divided the organisms into three distinct primary groups – the *urkingdoms* – on a more molecular level. The groups were categorized based on the sequences of the 16S (18S) ribosomal RNA genes, owing to the fact that these genes are highly abundant and easily accessible (Woese & Fox, 1977).

Later in 1990, Woese found that there was a group of anaerobic organisms (previously thought to belong to *Bacteria*) that was actually able to generate methane, which on the other hand, the *Bacteria* couldn't do. One of the other features that differs them from *Bacteria* is their N-linked glycoproteins (Allers & Mevarech, 2005). Consequently, Woese introduced and established a new classification of organisms - a new taxon called domain. The three domains being the highest level of classificaiton are the *Bacteria, Archaea* and *Eucarya* (see Figure 1) (Woese *et al*.,1990).

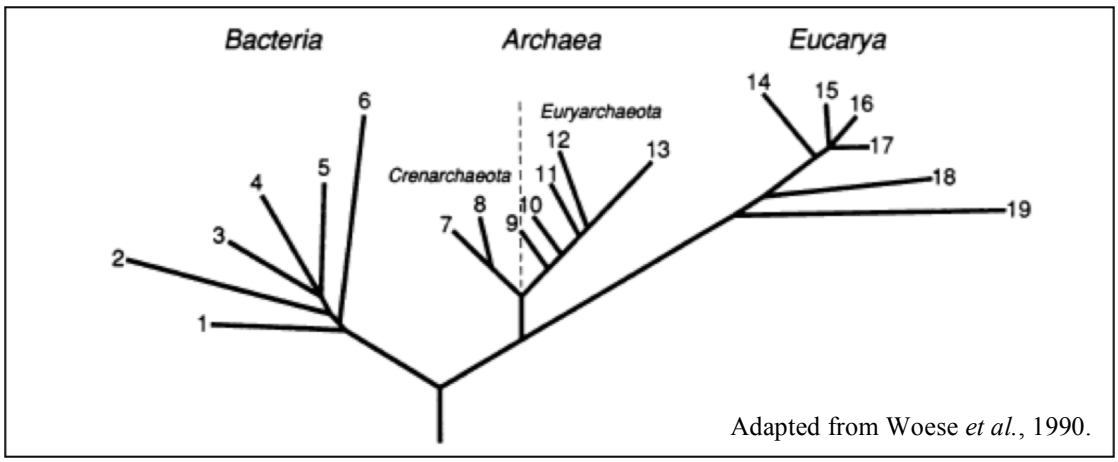

Figure 1. Carl Woese's representation of the phylogenetic tree.

This illustration depicts the three domains of life: *Bacteria*, *Archaea* and *Eucarya*, based on 16S (18S) rRNA sequence analysis. This phylogenetic tree also indicates the link between *Eucarya* and *Archaea* having a common ancestor (dotted lines). *Archaea* consists of two kingdoms: *Crenarchaeota* and *Euryarchaeota*.

1.2. *Archaea*

Archaea ("primitive" or "ancient" in Greek) represent one of the three domains of life and belong to the unicellular prokaryotic organisms. They were the first organisms to be described as extremophiles, adapted to living in such extreme environments such as hypersaline ponds or terrestrial hot springs. Nevertheless some of them also co-exist with both *Bacteria* and *Eucarya* in distinct environments, both terrestrial and aquatic, with high salinity, pressure and acidity, as well as in anaerobic surroundings (Rotschild & Mancinelli, 2001; Allers & Mevarech, 2005).

The classification of *Archaea* is divided into two main phyla: the *Euryachaeota* and the *Crenarchaeota* (see Figure 1) and three minor phyla based on sequence analysis taken from environmental samples: the *Korarchaeota*, the *Nanoarchaeota* and the *Thaumarchaeota* (Pikuta, 2011).

The *Euryachaeota* can further be divided into eight classes: *Archaeoglobi*, *Halobacteria*, *Methanobacteria*, *Methanococci*, *Methanomicrobia*, *Methanopyri*, *Thermococci* and *Thermoplasmata*. It is the most diverse group and contains all known methanogens, halophiles, hyperthermophiles and psychrophiles (Forterre *et al*., 2002; Gribaldo & Brochier-Armanet, 2006). Within these major phyla, methanogens are predominant (*Methanobacteria*, *Methanococci*, *Methanomicrobia* and *Methanopyri*) which are strict anaerobes generating methane by reducing carbon dioxide as fuel source (Bult *et al.*, 1996). Extreme halophilic species belong to the *Halobacteria*. These are able to grow both aerobically and phototropically. Due to the high molar concentrations of salt ions (4.5 M NaCl in their environment), high intracellular levels of KCl are required to control osmotic balance (Kennedy *et al*., 2001). Members of the *Archaeoglobi* are hyperthermophilic that can grow heterotrophically or chemilithoautotrophically with a neutral pH (Pikuta, 2011; Birkeland *et al*., 2017). *Thermococci* are extreme thermophilic, grow anaerobically and can be found in anoxic thermal waters. They best grow at 95°C with a neutral pH. However, *Thermoplasmata* are only moderately thermophilic and are highly acidophilic, which need a pH below 2 to optimally grow (Pikuta, 2011; Hogg, 2005).

The *Crenarchaeota* contains a unique class: the *Thermoprotei*, whose members are hyperthermophilic and acidophilic. They have been isolated from marine plankton, sandy ecosystems, deep sub-surfaces and freshwater samples (Schleper *et al*., 2005; Gribaldo & Brochier-Armanet, 2006). Their optimal growth temperature ranges between 60°C to 85°C. However, one of the most hyperthermophilic members, the *Pyrolobus fumarii*, grow at approximately 113°C in hydrothermal vents (Blöchl *et al*., 1997). They are also chemolithoautotrophic ammonia oxidizers, thus gaining their primary energy by oxidizing ammonia (Schleper *et al*., 2005).

The three minor phyla *Korarchaeota*, *Thaumarchaeota* and *Nanoarchaeota* could not be cultivated under laboratory conditions so far. The method used to study these is the analysis of their rRNA sequences derived from environmental samples (Barns *et al.*, 1996; Huber *et al.*, 2002; Brochier-Armanet *et al.*, 2008).

1.2.1. Characteristics of *Archaea*

Archaea can be seen as a mosaic of bacterial and eukaryotic features: On one hand, they resemble the macromolecular biosynthetic machinery of the *Eucarya* and on the other hand, their housekeeping functions are similar to that of the *Bacteria* (Berquist & DasSarma, 2003; Allers & Mevarech, 2005). For instance, *Archaea* contain histones similar to that of *Eucarya*, as well as proteins involved in transcription and translation, and the structure of the ribosome. Furthermore, some of the features they share with *Bacteria* are the circular chromosome, the small size of the genome and the polycistronic transcription units as well as the Shine-Dalgarno sequences found in the mRNA (Sarmiento *et al*., 2013).

In spite of the similarities *Archaea* share with the two other domains, they contain a special unique feature: their membrane lipids consist of branched isoprenoid acyl chains that are ether-linked to their glycerol backbone. In contrary, the membrane lipids in *Bacteria* and *Eucarya* are composed of ester-linked unbranched fatty acids (see Figure 2) (Kates, 1993; Jarrell *et al*., 2011). Ether linkages are vital in order for the *Archaea* to withstand high temperatures and extreme conditions (such as salinity), as they contribute a higher resistance towards hydrolysis. The membrane thus shows an increased stability, higher rigidity and increased tolerance to the surrounding (Van de Vossenberg *et al.*, 1999).

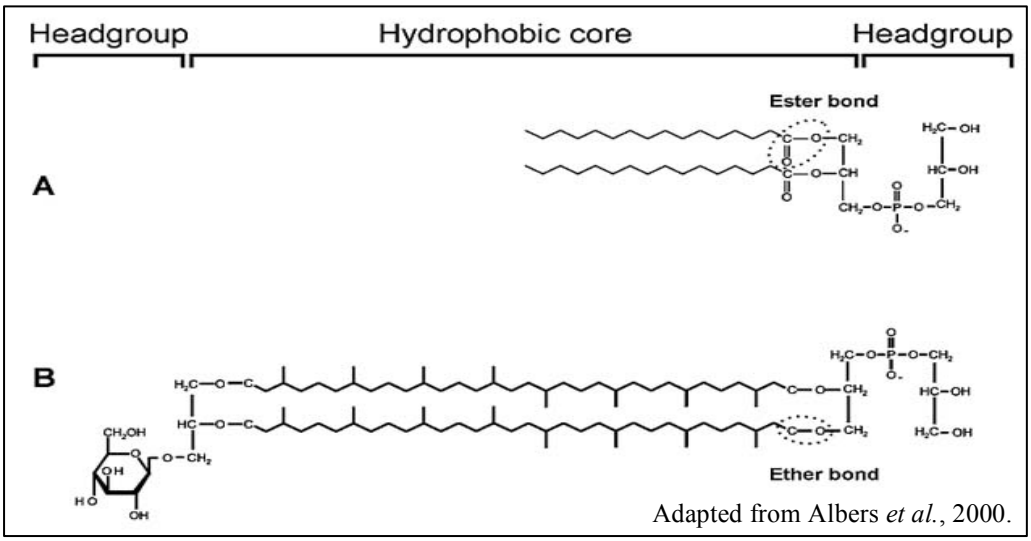

Figure 2. Membrane lipids of *Bacteria*, *Eucarya* and *Archaea*

(A) The unbranched fatty acid chains of *Bacteria* and *Eucarya* are ester-linked to the glycerol backbone.

(B) In *Archaea*, the branched isoprenoid acyl chains are ether-linked to the glycerol backbone.

The archaeal cell wall architecture can be quite intricate, due to the fact that there are a great variety of different cell wall structures as evident on Figure 3. The major groups of *Archaea* contain a cell wall composed of a pseudo-crystalline proteinaceous surface layer, the so-called S-layer, which is anchored to the cytoplasmic membrane. The glycosylation of the S-layer proteins increases thermal stability and thus hinders protein degradation (König *et al*., 2007; Yurist-Doutsch *et al.*, 2008; Albers & Meyer, 2011).

Moreover, pseudomurein, a polymer responsible for the maintenance of the cell shape, and thus the protection of the cells from osmotic pressure, exists in the methanogenic archaeal species *Methanothermus* and *Methanopyrus*, which lack the S-layer (König *et al*., 2007). It is very similar to the bacterial peptidoglycan that consists of *N*-acetylmuramic acid with a β-1,4 linkage to *D*-*N*-acetylglucosamine. However, the archaeal pseudomurein consists of *L*-*N*-acetyltalosaminuronic acid with a β-1,3 linkage to *D*-*N*-acetylglucosamine (Albers & Meyer, 2011).

Ignicoccus hospitalis also lack the S-layer in addition to the archaeal species mentioned above. Instead of the S-layer, an outer membrane is present, which shows similarity to that of the gram-negative bacteria (Klingl, 2014).

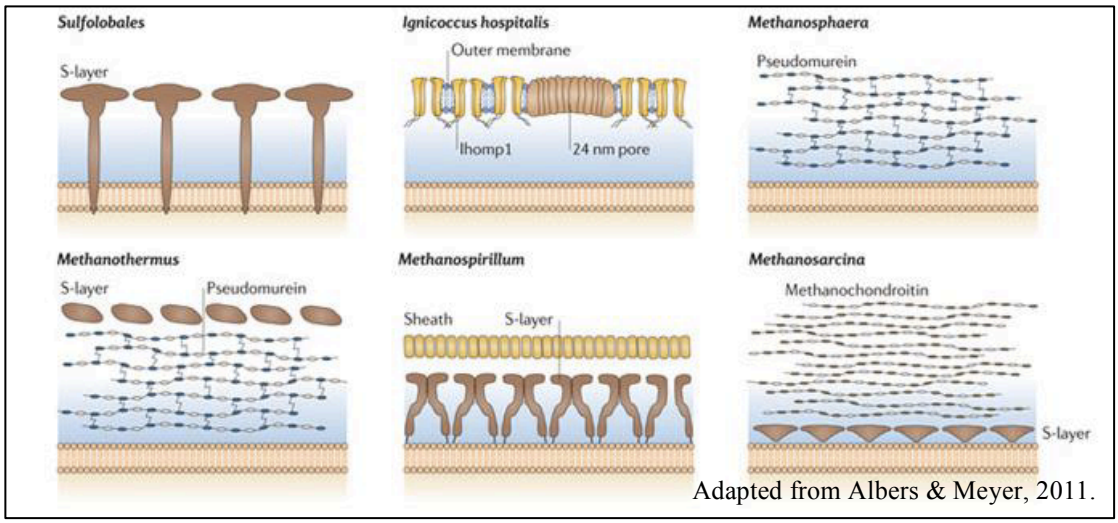

Figure 3. Distinct types of archaeal cell walls

The main type of archaeal cell wall is the S-layer, which is composed of a pseudo-crystalline proteinaceous surface layer that is anchored to the cytoplasmic membrane. *Ignicoccus hospitalis* and *Methanosphera* lack the S-layer. Moreover, *Ignicoccus hospitalis* contains an outer membrane, which is similar to that of the gram-negative *Bacteria*. *Methanosphera* however, is composed of pseudomurein.

1.2.2. Halophilic and haloalkaliphilic *Archaea*

One of the most substantial features of halophilic ("salt-loving") *Archaea* is their capability to thrive in environments with a high salt concentration. These salt-requiring microorganisms reside in hypersaline lakes in Africa or in the Dead Sea, and can also be found embedded in rocks in salt mines (Grant *et al*., 1998). The evaporation rates in these environments are higher than the precipitation rates and therefore lead to hypersalinity (Oren, 2002). Halophiles can be distinguished in diverse categories according to their salt tolerance: The extreme halophiles grow best in media with 2.5 – 5.2 M NaCl and the moderate halophiles require 0.5 – 2.5 M NaCl. Lastly, the halotolerants do not show an absolute necessity for salt, however they are able to tolerate high salt concentrations in their surroundings (Kushner & Kamekura, 1988).

Haloalkaliphilic *Archaea* require high salinity and high alkalinity for survival. They are mostly found in hypersaline soda lakes, many of which often have a bright red-purple color, such as the Lake Magadi in Kenya (Oren, 2002). The redness of these hypersaline lakes is caused by the red pigmentation in the membranes of the *Halobacteriaceae* due to the α-bacterioruberin (C-50 cartenoid pigment) and its derivatives. Owing to the fact that these habitats are mostly exposed to intense sunlight and high UV radiation, these haloalkaliphilic organisms have developed a system to repair DNA damage via bacterioruberin. This pigment is an antioxidant, and thus protects the DNA (Shahmohammadi *et al*., 1998).

1.2.2.1. Adaptations to high salt environments

As previously mentioned, halophilic and haloalkaliphilic *Archaea* are obliged to adapt and tolerate high salt concentrations in their surroundings in order for them to survive. To surpass the osmotic stress of these hypersaline environments, these microorganisms developed two different strategies: the "high-salt-in-strategy" and the "compatible solute strategy".

The "high-salt-in strategy" is based on the accumulation of potassium and chloride and allows these halophilic and halotolerant *Archaea* to prevent a rapid loss of water due to the presence of salt, thus maintaining their osmotically equivalent internal concentrations. In addition, they effectively pump out Na^+ ions using Na^+/H^+ antiporter systems. These organisms can therefore grow in media containing 3-4 M KCl or NaCl (Oren, 1999; Fendrihan *et al*., 2006).

The "compatible solute strategy" helps maintain the salt concentration in some of the halophilic and halotolerant organisms relatively low. They balance the osmotic potential by taking up or producing compatible solutes such as amino acids, amino acid derivatives, glycerol and sugars. In comparison to the previously mentioned strategy, this approach demands more energy (Oren, 1999; Roberts, 2005).

As for the haloalkaliphilic *Archaea*, they also require a high pH between 8 and 11 as well as a low Mg^{2+} concentration besides the high salt concentration. The majority of the enzymes require a neutral pH to perform their functions, and the intracellular pH therefore needs to stay neutral. This, again, is accomplished by the Na^+/H^+ antiporter systems (Van de Vossenberg *et al.*, 1999).

1.2.2.2. Halophilic and haloalkaliphilic proteins

Halophilic microorganisms developed adaptive mechanisms, in order to thrive in extreme conditions, such as in hypersaline environments. High salt concentrations usually alter the conformational stability of proteins. These microorganisms therefore require proteins that are also halophilic, in order to optimally function in high salt concentrations and low water availability (Allers, 2010). Halophilic proteins are generally unstable in environments with low salt concentrations, because they require salt to fold, for their stability and to prevent thermal denaturation (Reed *et al*., 2013). It has been shown that this haloadaption interacts with the surface structure of halophilic proteins, which contains acidic residues, such as glutamic and aspartic acids, and a low number of lysine (Tadeo *et al*., 2009). These acidic residues are suggested to commonly promote further protein hydration by generating a less hydrophobic surface, thus surviving the harmful outcome of the high salt concentrations and allowing the proteins to stay in solution (Reed *et al*., 2013).

However, to maintain a more neutral pH (ranging from 7 to 8.5) in the cytoplasm, haloalkaliphilic *Archaea* contain glycosylated proteins. The proteins of these haloalkaliphilic microorganisms also contain a high number of acidic residues, as seen in halophilic *Archaea* (Reed *et al*., 2013).

1.2.3. *Natrialba magadii*

Natrialba magadii is a haloalkaliphilic archaeon, which belongs to the family of *Halobacteriaceae* within the phylum *Euryarchaeota.* It was first discovered in and first isolated from Lake Magadi, Kenya in 1984 by Tindall *et al*. As mentioned in section 1.2.2., Lake Magadi is a hypersaline soda lake. It encompasses salt concentration up to 300 g/l, high levels of carbonate minerals and a pH above 11 (Oren, 2002). Ca^{2+} and Mg^{2+} can barely be detected, as they immediately precipitate at high pH and carbonate concentrations. Lake Magadi is regenerated by saline hot springs with temperatures reaching 86°C.

Upon discovery, *N. magadii* was previously classified in the genus *Nanobacterium* and called *Nanobacterium magadii*. However, after the 16S rRNA analysis and comparison to other species of the genus, it led to a new genus *Natrialba* and was finally named *Natrialba magadii* (Kamekura *et al*., 1997).

This archaeon is in need of high-salt concentrations between 3.5-4 M NaCl and a pH ranging from 9.5 to 11 for survival. Its optimal growth requires temperatures from 37-42°C as well as a Mg^{2+} concentration less than 10 mM (Siddaramappa, 2012). As soon as NaCl hits the concentration less than 2 M and the temperature sinks below 15°C, these may lead to the lysis of the cells. *N. magadii* is strictly aerobic and chemoorganotrophic, allowing it to gain its energy by oxidizing organic compounds.

N. magadii contains motile rod-shaped cells with a length of 5-7 µm and is polyploid consisting of up to 50 copies of chromosomal DNA per cell (Tindall *et al*., 1984). The generation time under laboratory conditions is approximately 9 hours in comparison to *E.coli* whose generation time is only about 20 minutes. This long generation time can be reasoned by the extreme conditions in the environment wherein it thrives and the amount of the chromosomal DNA copies per cell, all of which need to be replicated and eventually passed on to the daughter cells upon division.

1.2.3.1. Laboratory *N. magadii* strains: L11 and L13

There are two main strains that are being used in the laboratory: L11 and L13 (see Figure 4). *N. magadii* L11 is a lysogenic wildtype strain containing the virus ΦCh1, which terminates its life cycle through lysis of the host cell. However, the *N. magadii* L13 is a non-lysogenic strain, lacking the prophage through repeated cell culture passaging, hence being called the "cured" strain. This "cured" *N. magadii* L13 however, may still be re-infected by ΦCh1 and is therefore used as the indicator strain for studying ΦCh1. Up to this date, *N. magadii* is the only known host of ΦCh1. (Witte *et al*., 1997).

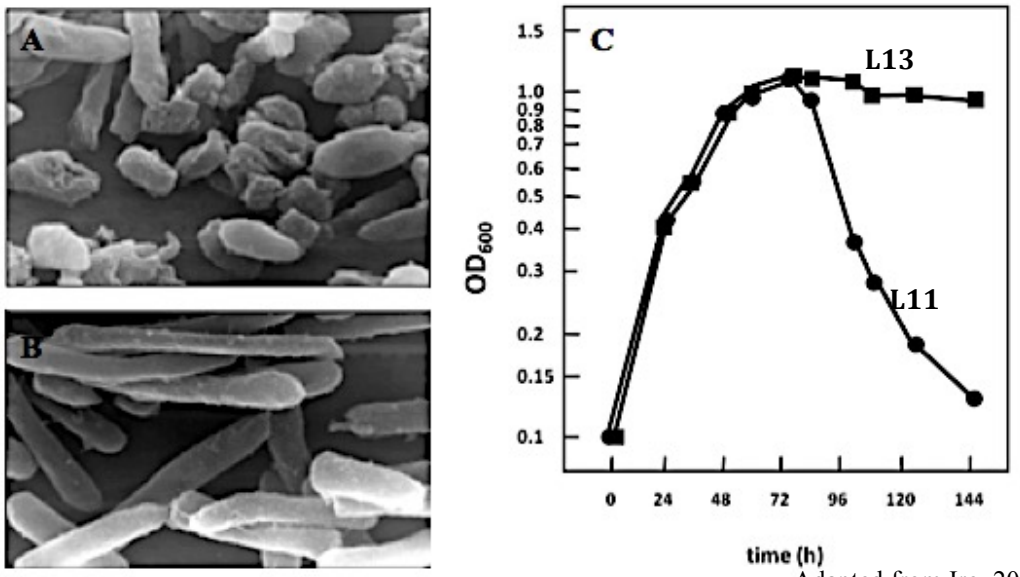

Adapted from Iro, 2006.

Figure 4. Electron micrographs and growth kinetics of *N. magadii* L11 and *N. magadii* L13

(A) *N. magadii* L11, the wildtype strain carrying ΦCh1 as a prophage. Lysed cells can be observed, as ΦCh1 is a lysogenic virus, terminating its life cycle through lysis of the host cell.

(B) *N. magadii* L13, the cured strain. Healthy rod-shaped cells are evident.

(C) The graph depicts the growth kinetics of both strains and illustrates that their exponential growth behaviors are almost identical. However, the virus-induced lysis of *N.magadii* L11 occurs after approximately three days. As for *N. magadii* L13, no lysis can be observed.

1.2.3.2. Genetic alterations of *N. magadii*

The high copy numbers of chromosomes (50 copies), the long generation time (9 hours) and the limited selection markers as well as shuttle vectors are one of the main reasons for the complex and challenging handling of *N. magadii*. Taking these into considerations, it takes time to perform genetic manipulations in *N. magadii*.

1.2.3.2.1. Transformation

Cline and Doolittle were the first to successfully transform *Archaea* in 1987. They used the isolated DNA from the halophage ΦH to transfect the extremely halophilic *Halobacterium halobium* and performed plaque assay to analyze the transformation efficiency (Cline & Doolittle, 1987). The method applied for transfection is based on polyethylene glycol 600 (PEG 600) and the generation of spheroplasts is achieved by using EDTA, thus removing the S-layer. However, as for the transformation of *N. magadii*, EDTA was proven not to be sufficient to remove the S-layer, and therefore the *N. magadii* cells were treated with bacitracin that prevents glycosylation of the S-layer. In addition, enzymatic digestion by proteinase K was used to further increase the sufficiency of the removal of the S-layer (see Figure 5). This approach generated spheroplasts, which were capable to take up purified DNA of ΦCh1 (Mayrhofe-Iro *et al*., 2013). To regenerate the cells, they were incubated at 37°C.

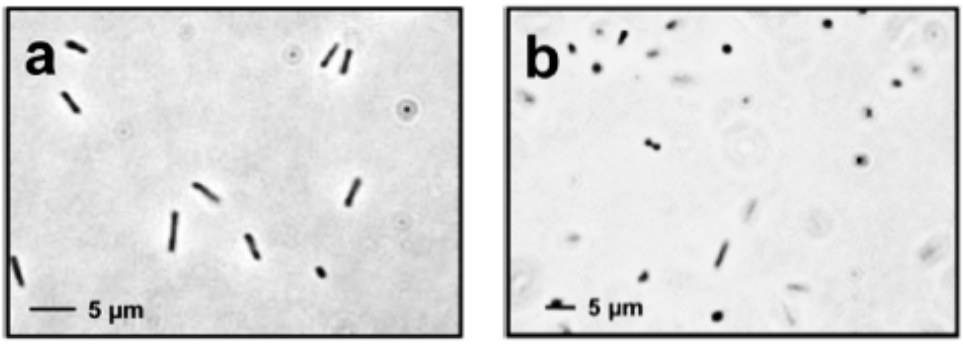

Adapted from Mayrhofer-Iro *et al*., 2013.

Figure 5. Micrographs of spheroplasts of *N. magadii* L13.

(a) *N. magadii* cells grown in rich medium and are rod-shaped.

(b) *N. magadii* cells start rounding whilst being treated with bacitracin and proteinase K, as they lose the S-layer. After regenerating for about 48 hours at 37°C, the cells become rod-shaped again.

1.2.3.2.2. Selection markers and shuttle vectors

In order to perform genetic alterations in *Archaea*, it is necessary to create different shuttle vectors. Up until now there are only two frequently used shuttle vectors for transformations in *N. magadii*: pRo-5 and pNB102 (see Figure 6).

The plasmid pRo-5 is based on the *E. coli* vector pKS_{II}^{+}, which contains the point-mutated *gyrB* gene from the halophilic archaeon *Haloferax alicantei*, thus providing a novobiocin resistance as selection marker for *N. magadii* (Mayrhofer-Iro *et al.*, 2013). Novobiocin is a DNA gyrase inhibitor that blocks the ATP-binding site, thus also inhibiting cell growth (Holmes & Dyall-Smitt, 1991). In addition, a *bla* resistance marker is also present in pRo-5, generating a supplementary ampicillin resistance for selection in *E. coli*. It also contains different parts of ΦCh1 ORF 53 and ORF54 that serve as origin of replication to carry out autonomous replication in *N. magadii* (Mayrhofer-Iro *et al*., 2013).

The plasmid pNB102 results from the plasmid pNB101. Plasmid pNB102 contains the ColE1 origin of replication of *E. coli* .Two selection markers are incorporated in this plasmid: ampicillin and mevinolin (Zhou *et al*., 2004).

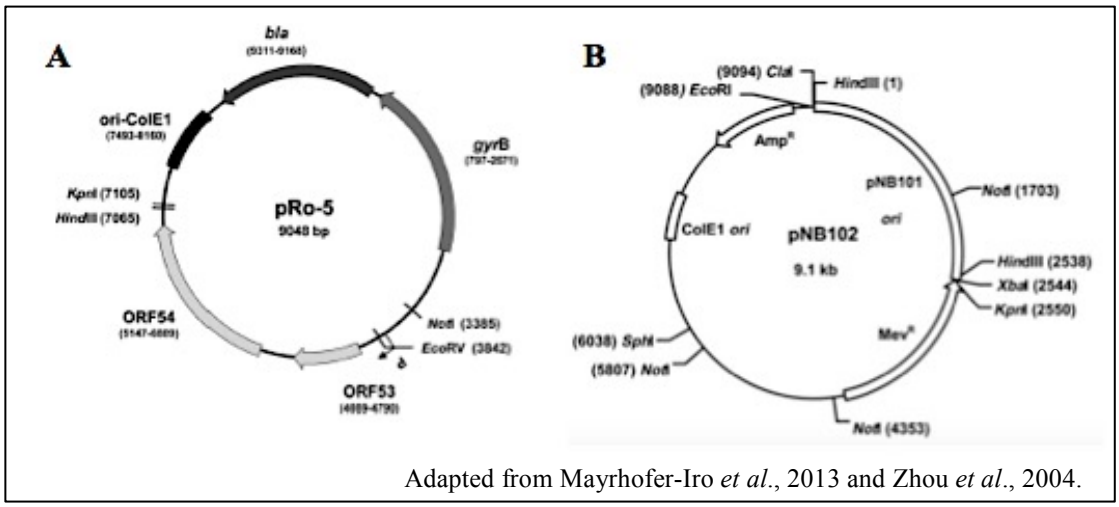

Adapted from Mayrhofer-Iro *et al*., 2013 and Zhou *et al*., 2004.

Figure 6. Shuttle vectors of *N. magadii*.

(A) Shuttle vector pRo-5 carrying the selection markers: novobiocin resistance for *N. magadii* and ampicillin resistance for *E .coli*.

(B) Shuttle vector pNB102 carrying the selection markers: mevinolin resistance for *N. magadii* and ampicillin resistance for *E .coli*.

1.3. Viruses of *Archaea*

Almost all different forms of life are subject to viral infections, however so far, not all viruses have been identified. Up to this date, only approximately 50 viruses have been reported to infect *Archaea* (Prangishivili, 2006). Most of the archaeal viruses have been isolated from different environments, wherein archaeal organisms are dominant. These environments include extreme thermal, saline and acidic surroundings (Sorek *et al*., 2008). Viruses serve as great model systems to illustrate both their own genetics as well as various genetic mechanisms of their hosts. According to many virologists, archaeviruses can further be recognized as bacteriophages, regardless of the fact that they have nothing in common with those bacteriophages infecting *Bacteria* (Abedon & Murray, 2013). The first discovered archaeviruses were those infecting

Halobacterium cutirubrum and *Halobacterium salinarium* (Torsvik & Dundas, 1974; Wais *et al*., 1975). The best-studied archaeviruses are the ΦH infecting *H. salinarium* and ΦCh1 infecting *N. magadii*. ΦCh1 is closely related to ΦH and Witte *et al*. first characterized it in 1997 (Dyall-Smith *et al*., 2003; Witte *et al*., 1997).

1.3.1. The haloalkaliphilic virus ΦCh1

As previously mentioned, Witte *et al*. were the first to discover and subsequently isolate the virus ΦCh1. The isolation resulted from a preliminary observation that batch cultures of *N. magadii* spontaneously started lysis as soon as it reached the stationary growth phase. The phage particles of ΦCh1 were collected from the supernatant of the culture. It has been proven that the re-infection of the strain *N. magadii* L11, from which the virus particles were isolated, was not possible. However, only *N. magadii* that was cured of viruses – the strain *N. magadii* L13 – via repeated cell culture passaging as mentioned on section 1.2.3.1. was able to be infected with the bacteriophage ΦCh1 resulting in its lysis (Witte *et al*., 1997).

ΦCh1 is a temperate virus, which belongs to the family of the *Myoviridae*, and is hitherto the only haloalkaliphilic bacteriophage isolated (Witte *et al*., 1997). It shares a sequence identity of 97% with its closest relative ΦH infecting *H. salinarum* (Dyall-Smith *et al*., 2003). Nevertheless, their main difference lies in their methods of invading their host cells: ΦH acts as an episomal prophage in *H. salinarum*, when in fact ΦCh1 is integrated into the host chromosome, thus acting as an integrated prophage (Schnabel & Zillig, 1984; Witte *et al*., 1997). As evident on Figure 7, ΦCh1 is a typical head-tail virus, which is typical for the representatives of *Myoviridae*. Its length is approximately 200 nm, with an icosahedral head (70 nm) carrying the viral genome of 58498 bp and a contractible tail (130 nm), which is 20 nm wide. Structures at the end of the virus tails are supposedly in charge of adsorption.

Furthermore, the mature viral particle contains various RNA species, ranging between 80 and 700 nucleotides in length. The virion-associated RNA has been reported to be host-encoded (Witte *et al*., 1997).

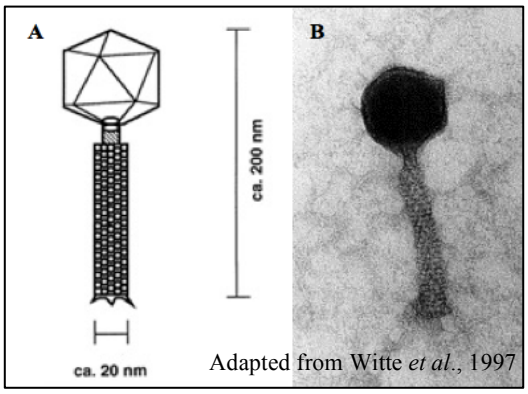

Figure 7. Illustrations of the head-tail ΦCh1 virus.

(A) Schematic drawing of ΦCh1 with the icosahedral head and the contractible tail.

(B) Electron micrograph of ΦCh1.

Just like the conditions their host thrives in, high salt concentration is significant for both the infectivity and the stability of ΦCh1. As per Witte *et al*., salt concentrations lower than 2 M NaCl, seemingly lead to the dissociation of the virus particles or conformational changes of the capsid proteins, thus resulting to an accelerated loss of infectivity (Witte *et al*., 1997). It has been revealed that ΦCh1 contains four major (A, E, H and I) and five minor proteins (B, C, D, F and G), which have a size ranging from 15-80 kDa and were supposedly mainly acidic, thus having isoelectric points between pH 3.3 and pH 5.2 similar to various proteins of other halophilic *Archaea* (Lanyi, 1974).

Observations that the DNA of ΦCh1 is partially methylated were also addressed. Partial resistance to the restriction of ΦCh1 via *Eco*RV was observed, indicating that some bases were presumably modified. The DNA of *N. magadii* is partially Dam-like methylated at the adenine residues, which led to the observation that ΦCh1 might code for its own methylation. After further analysis, the methyltransferase M.*Nma*ΦCh1I was discovered (Baranyi *et al*., 2000).

The first nucleotide sequence of ΦCh1 was established by Klein *et al*. in 2002 describing 98 distinct open reading frames (ORF), which were concluded to be protein-coding genes. Only four of the ORFs (3, 41, 79 and 83) start with GTG, whereas the rest of the ORFs start with ATG. As previously mentioned, ΦCh1 genome consists of 58498 bp with an overall G+C content of 61.9%. The linear genome (dsDNA) of ΦCh1 (see Figure 8) is organized into three parts: On the left side (ORFs 1-34), genes coding for structural proteins are present. These genes are presumably involved in virion morphogenesis. In the mid-section (ORFs 35-55), genes responsible for replication functions, gene regulation and plasmid stabilization, can be found. The right part contains genes whose functions are still quite unknown, as well as genes coding for DNA methylation and restriction (Klein *et al*., 2002). This type of genome organization into functional modules mirrors those of other double-stranded bacteriophages with head-tail morphology. It has been shown that the central part of ΦCh1 genome is similar to the L-segment (pΦHL) of the virus ΦH, which can circularize and replicate independently on its own. ΦCh1 differs from ΦH by not having insertion sequences (IS). Possible reason for the presence of IS elements in ΦH is due to the fact that *H. salinarum*, the host of ΦH, thrives in a neutral pH for survival and contains many different sequences (Schnabel & Zillig, 1984; Klein *et al*., 2002). Regardless of the similarities ΦCh1 and ΦH share, it was proven that ΦCh1 is not able to infect *H. salinarum* cells, thus not including *H. salinarum* as its host. Up to this date, *N. magadii* is the only known host of ΦCh1 (Witte *et al*., 1997).

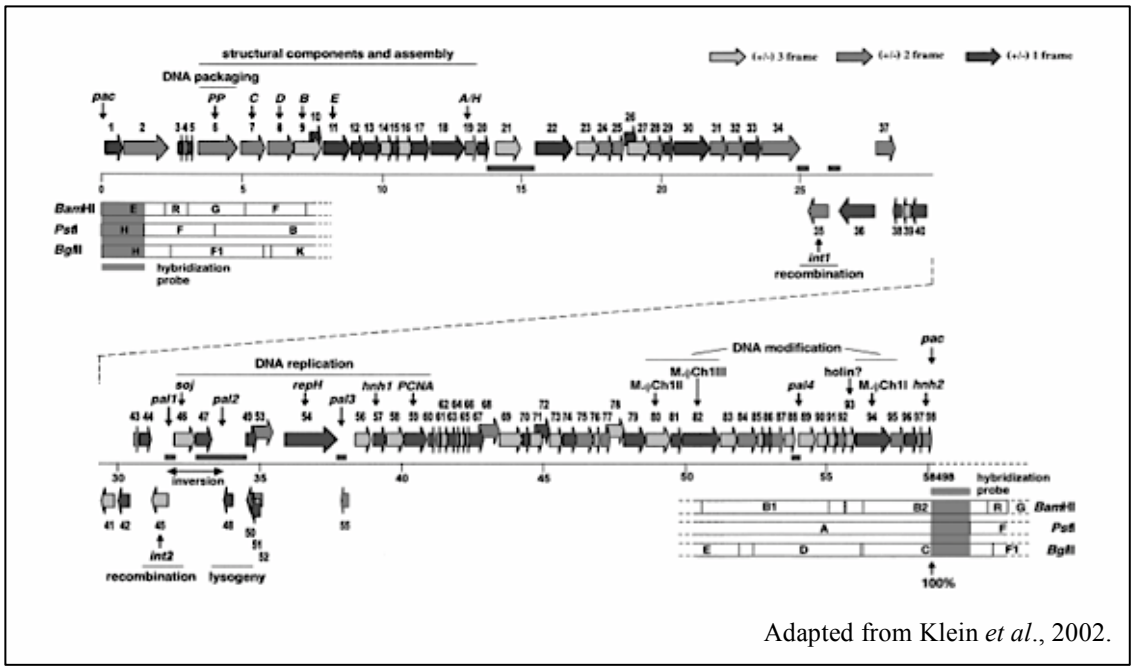

Adapted from Klein *et al*., 2002.

Figure 8. Illustration of the linear 58498 bp genome of ΦCh1 with the 98 ORFs.

The ORFs are represented by arrows, and the putative, along with the established functions of the gene products, are shown. The genome consists of three functional modules: On the left side, the genes coding for structural proteins, which are presumably involved in virion morphogenesis, are present. The central part is involved in replication, regulation of gene expression and plasmid stabilization. The genes on the right side are responsible for DNA modification. Most of the genes responsible for DNA modification, however, still have unknown functions, except for the three discovered ΦCh1 methyltransferases: the ORF94-encoded methyltransferase M.*Nma*ΦCh1I, M.*Nma*ΦCh1II and M.*Nma*ΦCh1III.

1.4. ORF44

1.4.1. ΦCh1 ORF43/44 as a putative VapBC toxin-antitoxin system

1.4.1.1. Toxin-Antitoxin System in general

Toxin-antitoxin (TA) modules were initially classified as plasmid maintenance or stability modules (Holcik & Iyer, 1997). TA systems have then been described to protect against DNA loss, thus serving as protection against DNA invasion (Van Melderen, 2010). They also partake in stress regulation via apoptosis or by persister formation, which allows the cells to tolerate antibiotics (Lewis, 2010). Essentially all

Bacteria and a number of *Archaea* have genes, which produce proteins that prevent cell growth and eventually lead to apoptotic cell death. A gene encoding a small toxin protein belongs to this TA system and can prevent cell growth by targeting substances that participate in fundamental cellular processes, such as DNA replication, mRNA stability and protein synthesis (Pandey & Gerdes, 2005; Yamaguchi *et al*., 2011). These toxins are co-transcribed and co-translated with their counterpart – the antitoxins – and together they build the TA operon. The TA operon is a stable complex, which can be found in normally growing cells, wherein the cognate antitoxin is continuously synthesized, in order to inhibit and neutralize the toxicity that the toxin carries (Yamaguchi & Inouye, 2009). Generally, toxins are more stable than their corresponding antitoxin, which get easily degraded under stress conditions such as after phage infection, leading to the toxic effects of the toxins, as the antitoxins are no longer able to inhibit their counterpart (Yamaguchi *et al*., 2011). Toxins are very resistant to proteases and their toxic effects include acting as endoribonucleases as well as inhibitor of translation initiation or elongation, and also cause defects in cell wall synthesis (Bailey & Hayes, 2009; Mutschler *et al*., 2011). All these, in turn, lead to cell killing, followed by reduced phage spreading.

There are three types of TA systems: The antitoxins in type I and III TA systems are small noncoding RNAs, which bind to the toxin mRNA and prevents the toxin production. Type II TA system contains unstable antitoxin protein, which binds to the toxin and inhibits it (Van Melderen & Saavedra De Bast, 2009).

1.4.1.2. Indications for a potential VapBC toxin-antitoxin system

The locus of ORF44 is upstream of the ΦCh1 replication domain, and together with ORF43, it forms an operon. Both ORFs have overlapping start and stop codons, which means that they are both co-transcribed and co-translated. It is known that domain fusions are indicative of functional linkages between domains (Marcotte *et al*., 1999).

It was reported that gene products of ORF43 (gp43) and ORF43/44 (gp43/44) transformed in the halophilic model organism *Haloferax volcanii* have an enhancing effect on ORF49 by directly or indirectly binding to the 5' repeats in the ORF48 (*rep*) sequence. ORF48 and ORF49 represent a repressor-operator system, making up the lysogenic region of ΦCh1. Iro *et al*., performed experiments that suggest that ORF49 is presumably involved in the activation of the lytic life cycle: The gene product of ORF49 is conceivably involved in the shifting between lysogenic and the lytic life cycle. However, it may also encode a factor that accelerates the progression to the lytic cycle. It was also demonstrated that gp44 alone abolishes the enhancing effect and can therefore be considered as a repressor molecule (Iro *et al*., 2007).

Further experiments were performed and after Pfam analysis, a PIN domain in the ORF44 gene product gp44 was revealed. PIN domains generally cleave single-stranded RNA in a sequence-specific, Mg^{2+} or Mn^{2+}-dependent, manner (Arcus *et al*., 2011). These ribonucleases are reported to be toxic to the cells that express them, thus representing the toxins of the TA systems. PIN domain TAs have been named VapBC (virulence associated proteins B and C) TAs, wherein VapB is the inhibitor, which contains a transcription domain and VapC is the PIN domain ribonuclease. VapBC TA system belongs to type II TAs, wherein the downstream gene generally represents the toxin (VapC) and the upstream gene the antitoxin (VapB) (Van Melderen and Saavedra De Bast, 2009). In 2011, Arcus *et al*. showed that the VapBC complex autoregulates its own expression, wherein VapC becomes active, as soon as the VapB is degraded (see Figure 9). Since gp44 contains a PIN domain, the hypothesis claiming gp44 to be the putative toxin of this TA system and ORF43 to be the putative antitoxin, arose.

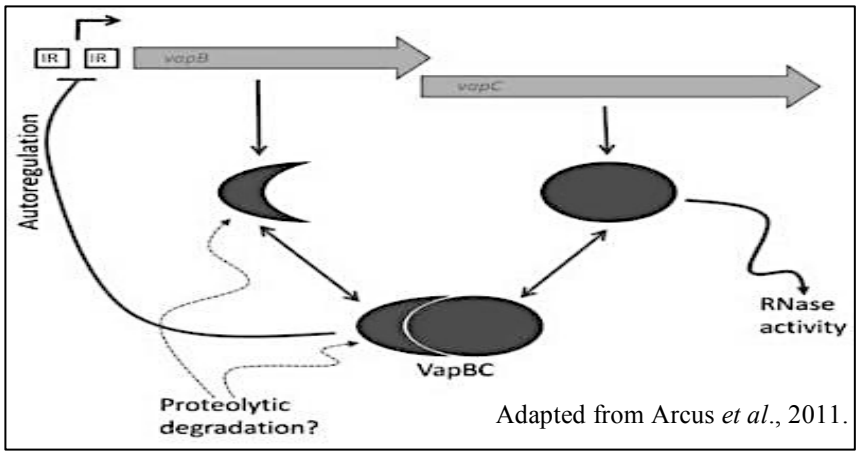

Figure 9. VapBC toxin-antitoxin system.

The two overlapping genes contained in this TA system are organized in an operon.

The VapBC complex consists of the instable VapB (antitoxin) and the stable VapC (toxin).

As soon as the antitoxin is degraded, the toxin becomes active.

In 2015, Hofbauer performed experiments in the cured strain *N. magadii* L13 approaching the characterization of ORF43/44. The effects of ORF43 and ORF44 on the expression of $ORF34_{52}$ (coding for tail-fibre protein) in *N. magadii* L13 were analyzed. ORF43 and ORF44 were individually cloned into the construct containing the promoter p43 and the chosen reporter gene ($ORF34_{52}$). The *N. magadii* L13 strain with ORF44 alone resulted in the production of a truncated tail-fibre protein (see Figure 10 A), indicating that this truncation may be due to the putative RNase function induced by gp44.

The next experiment with ORF43 and ORF44 was then performed using the ORF94 (coding for methyltransferase) as the reporter gene. As evident on Figure 10 B, there was a 48-hour delay in reporter gene expression containing ORF44 under the control of p43. There was no shortened protein, but a weaker expression of ORF94, indicating that gp44 may not have cleaved the coding sequence of ORF94, but conceivably the upstream region.

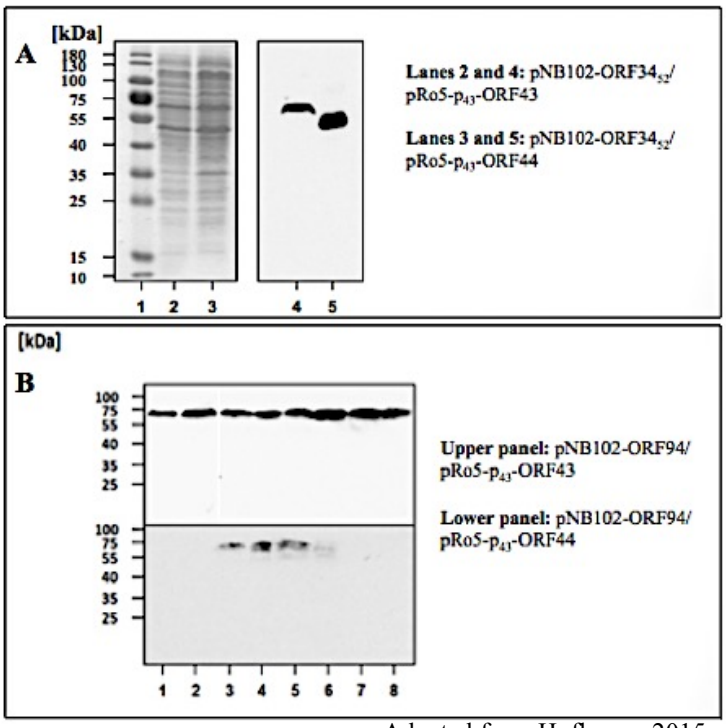

Adapted from Hofbauer, 2015.

Figure 10. Effects of ORF44 on the expression of ORF34$_{52}$ and ORF94 in *N. magadii* L13.

(A) ORF44 alone causes production of a truncated tail-fibre protein (gp34$_{52}$), in comparison to the strain with only ORF43. The putative RNase gp44 may have cleaved the coding sequence of ORF34$_{52}$, thus generating a shorter protein, which is approximately 20 kDa shorter than that generated by solely ORF43.

(B) A 48-hour delay in the expression of ORF94 is evident on the lower panel containing exclusively ORF44. Furthermore, the generated proteins are equal in size, indicating that there was no truncation. This indicates that the coding sequence of ORF94 was not cleaved, but most probably the upstream region.

An "EMBOSS Water Pairwise Sequence Alignment" (https://www.ebi.ac.uk/Tools/psa/emboss_water/nucleotide.html) analysis was performed to compare the coding sequence of ORF34 and the upstream region of ORF94 (see Figure11). The analysis shows a huge similarity in the sequences. This indicates that gp44, having a PIN domain, may cleave RNAs in a sequence-specific manner, as aforementioned.

These preliminary results therefore suggest a putative regulating function of gp44 as a putative RNase.

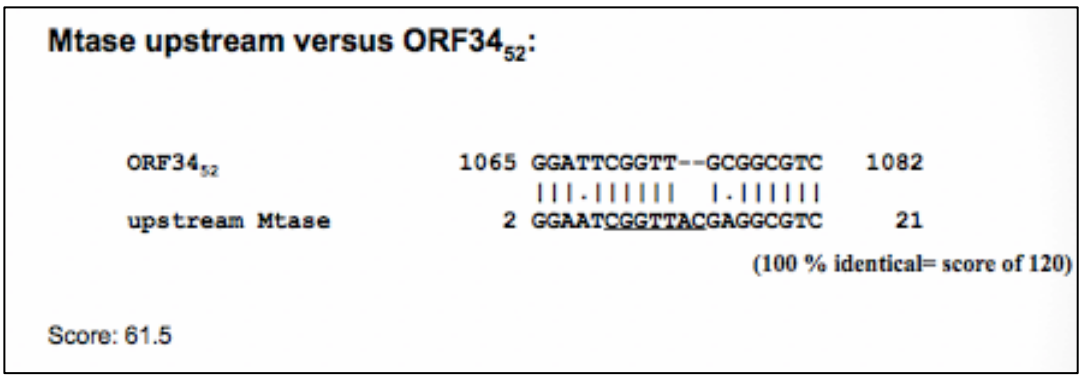

Figure 11. Sequence alignment of the coding sequence of ORF34$_{52}$ and the upstream region of ORF94.

The coding sequence of ORF34$_{52}$ (coding for tail-fibre protein) and the sequence of the upstream region of ORF94 (coding for methyltransferase) are significantly similar. This shows that gp44 may have an effect on these similar sequences, thus supposedly cleaves in a sequence-specific manner.

In addition, a deletion strain of ΦCh1, ΦCh1::ORF44, wherein the putative toxin-encoding gene of ΦCh1 was replaced by a novobiocin resistance cassette, showed a more rapid loss of the provirus as detectable in the wild type. Prophages generally act as only temporary passengers on the bacterial chromosomes. There were theoretical arguments suggesting a series of events, which resulted from the accumulation of mutations to enormous loss of prophage DNA and eventual disappearance of the prophage (Canchaya *et al*., 2003; Lawrence *et al*., 2001). This scenario is supported by various observations. Many prophages are not inducible any more (Ventura *et al*., 2003). Inactivating point mutations were occasionally determined by bioinformatic analysis, such as the introduction of stop codons into the replisome organizer gene and the portal protein-encoding gene in *Streptococcus pyogenes* prophages SF370.2 and SF370.3 (Desiere *et al*., 2001) or inactivation of the N-antitermination genes in the lambdoid coliphages from O157 (Lawrence *et al*., 2001).

2. Materials and Methods

2.1. Materials

2.1.1. Strains

2.1.1.1. *E. coli*

Strain	Genotype	Source
Lemo21 (DE3)	*fhuA2 [lon] ompT gal (λDE3) [dcm]* Δ*hsdS/pLemo*(Cam^R) *λ DE3 = λ sBamHIo* Δ*EcoRIB int::(lacI::PlacUV5::T7 gene1) i21* Δ*nin5* pLemo = pACYC184-*PrhaBAD-lysY*	BioLabs
Tuner	*F-, ompT, hsdSB (rB^-mB^-), gal, dcm, lacY1*	Novagen
XL1-Blue	*recA1, endA1, gyrA96, thi, hsdR17*(r_K^-, m_K^+), *supE44, relA1, lac, [*F′*, proAB*+, *$lacI_qZ$*Δ*M15,* Tn10*(*Tet_r*)]*	Stratagene

2.1.1.2. *N. magadii*

Strain	Genotype	Source
L11	Wild type strain carrying provirus φCh1	Witte *et al.*, 1997
L13	φCh1 cured derivate of L11	Witte *et al.*, 1997

2.1.2. Growth media

Lysogeny broth (LB) medium for *E. coli*

Peptone	10 g
Yeast Extract	5 g
NaCl	5 g
pH 7.0	
add ddH_2O to 1 l	
15 g/l agar for agar plates	

NVM^+ - rich medium for *N. magadii*

Casamino acids (Casein hydrolysate)	8.8 g
Yeast extract	11.7 g
Tri-Na citrate 0.8 g	
KCl	2.4 g
NaCl	235 g
pH 9 – 9.5	
add ddH_2O to 935 ml	
8 g/l agar for agar plates	
4 g/l agar for soft agar	

After autoclaving, the medium or agar was complemented by adding:

0.57 M Na_2CO_3	65 ml
1 M $MgSO_4$	1 ml
20 mM $FeSO_4$	1 ml

2.1.3. Antibiotics and additives

Compound	Stock concentration	Final concentration	Preparation
Ampicillin	20 mg/ml	100 µg/ml	dissolved in ddH_2O, sterile filtered, storage at 4°C
Bacitracin	3 mg/ml	70 µg/ml	dissolved in ddH_2O, sterile filtered, storage at 4°C
Chloramphenicol	40 mg/ml	20 µg/ml	dissolved in 96% EtOH, storage at -20°C
IPTG	1 M	0.4 mM	dissolved in ddH_2O, sterile filtered, storage at -20°C
Kanamycin	25 mg/ml	50 µg/ml	dissolved in ddH_2O, sterile filtered, storage at 4°C
L-rhamnose	1 M	1 mM	dissolved in ddH_2O, sterile filtered, storage at -20°C
Mevinolin	10 mg/ml	7.5 µg/ml	stock solution prepared from commercially available tablets, light protection, dissolved in 96% EtOH, storage at -20°C
Novobiocin	7 mg/ml	3 µg/ml	dissolved in ddH_2O, sterile filtered, storage at -20°C
Tetracycline	10 mg/ml	10 µg/ml	dissolved in half of EtOH and half ddH_2O, stored at -20°C

2.1.4. Primers

Primer Name	Sequence	Tm in °C	Restriction site(s)
34-3	CAGCAGAAGCTTCAGATCAGGTTTATATTGCTGAAGT	60.2	*Hind*III
34-D-5	CAGGAGATCTATGCCGCGAAGTGCG	65.0	*Bgl*II
36-3	GACGAGATCTCGAGACGGCAGCAACG	64.5	*Bgl*II
36-D-5	GACGGGATCCATGGCGGTCGGGAAGT	60.0	*Bam*HI
43-3	CAGCAGTCTAGACGTGTCGACGAACAGC	58.7	*Xba*I
43-5	CAGCAGTCTAGACGTTGTGCCAGCCGT	62.1	*Xba*I
43-Kpn-5	CAGCAGGTACCGTTGTGCCAGCCGT	60.0	*Kpn*I
44-3-Xba	CAGCTCTAGATGATTTAGGACTCGAGGACC	68.1	*Xba*I
44-Hind	CAGCAAGCTTGATTTAGGACTCGAGGACC	56.4	*Hind*III
56-3	CAGCGTCTAGACTGCAGTCACTGCTGACCACCGG	53.0	*Xba*I, *Pst*I
56-5	CAGCAGGATCCATGAGAGAGAACAATCC	49.0	*Bam*HI
MT-Kpn-5	GAATGGTACCGCGAGTCGGACAACGTTC	63.4	*Kpn*I
MT-M-Kpn	GAATGGTACCGCGAGTCGGACAACGTTCACTGAGTCGAGTCACCCCACTGAACGCAGATACCAGCTGTGTTCGGTCGAACCACCAGGGAAGAATTCACGAGGCGTCACGATGC	77.0	*Kpn*I
MT-Xba-3	GATCTCTAGATCACTCATTATCACCGGCGT	64.2	*Xba*I
TR-1X	AATTTCTAGACCGCGTTGAAGGCAGCT	66.6	*Xba*I
TR-2	AATTTCTAGATCCTGGGCCTCTTTGAA	60.7	*Xba*I

2.1.5. Plasmids

Construct	Features	Source
pNB102	*bla*, ColE1 ori, *hmg* (Mev^R), pNB101 ori	Zhou *et al*., 2004
pREP4	F^-, *mcr*A, Δ(*mrr-hsd*RMS-*mcr*BC), Φ80*lac*ZΔM15, Δ*lac* 74 *rec*A1, *ara*D139, Δ(*ara-leu*)7697, *gal*U, *gal*K, *rps*L (Str^R), *end*A1, *nup*G	Invitrogen
pRo-5	*bla*, gyrB (Nov^R), ColE1 ori, ΦCh1 ori	Mayrhofer-Iro *et al*., 2013
pRSET-A	*bla*, pUC ori, T7 promoter, N-terminal 6x His-tag	Invitrogen
pKSII-ΔORF44-1-4-Nov^R-R	pBlueScript II KS(+) containing upstream and downstream regions of ΦCh1 ORF44 flanked by a novobiocin resistance cassette in reverse orientation	Gillen, 2017
pNB102-ORF94-M2	pNB102 containing ΦCh1 ORF94 (Methyltransferase), *Eco*RI restriction site introduced into the upstream region.	This study
pNB102-ORF94	pNB102 containing ΦCh1 ORF94 (Methyltransferase)	Hofbauer, 2014
pNB102-p43-43/44	pNB102 containing a ΦCh1 ORF43/44 under a ΦCh1 ORF43 promoter	Till, 2010
pNB102-p43-44	pNB102 containing ΦCh1 ORF44 under a ΦCh1 ORF43 promoter	This study
pREP4-pRSETA-ORF44	pREP4 containing pRSETA-ORF44	This study
pRo-p43-43	pRo-5 containing ΦCh1 ORF43 under a ΦCh1 ORF43 promoter	Meissner, 2008

pRo-p43-43/44	pRo-5 containing ΦCh1 ORF43/44 under a ΦCh1 ORF43 promoter	Meissner, 2008
pRo-p43-44	pRo-5 containing containing ΦCh1 ORF44 under a ΦCh1 ORF43 promoter	Meissner, 2008
pRSET-A-34	pRSET-A containing ΦCh1 ORF34	This study
pRSET-A-36	pRSET-A containing ΦCh1 ORF36	This study
pRSET-A-ORF44	pRSET-A contatining ΦCh1 ORF44	Iro, 2006

2.1.6. Enzymes

All enzymes were used in combination with their appropriate buffers, as recommended by the company.

Enzyme	**Company**	**Product Number**
Restriction enzymes	Thermo Scientific	-
DNA Polymerases		
Pfu DNA Polymerase	Promega	M7741
DreamTaq Polymerase		
Go*Taq* DNA Polymerase/Mastermix	Promega	M3001/M7123
DNA modifying enzymes		
T4 DNA ligase	Promega	M1801
DNA in vitro transcription		
AmpliScribe T7-*Flash* Enzyme Solution	Epicenter	ASF3257/ASF3507
Other enzymes		
Lyozyme from chicken egg white	Sigma	L6876
Proteinase K	Qiagen	1019499

2.1.7. Nucleotides

Name	Company	Product Number
dNTP Mix	Promega	U1511
ATP	Epicentre	ASF3257/ASF3507
CTP	Epicentre	ASF3257/ASF3507
GTP	Epicentre	ASF3257/ASF3507
UTP	Epicentre	ASF3257/ASF3507

2.1.8. DNA/RNA and protein markers

DNA/RNA ladder	Company	Size range in bp
Lambda DNA *Bst*EII Digest	Thermo Scientific	702, 1264, 1371, 1929, 2323, 3675, 4324, 4822, 5686, 6369, 7242, 8454
GeneRuler 1kb DNA Ladder	Thermo Scientific	250 to 10000
GeneRuler 100 bp	Thermo Scientific	100 to 3000
Protein ladder	**Company**	**Size range in kDa**
PageRuler™ Prestained Protein Ladder	Thermo Scientific	10, 15, 25, 35, 40, 55, 70, 100, 130, 170

2.1.9. Kits

Name	Company	Product Number	Usage
AmpliScribe™ T7-Flash™ Transcription Kit	Epicentre	ASF3257/ASF3507	*In vitro* transcription
Clarity™ Western ECL Substrate	BioRad	170-5061	Western Blot - Chemiluminescence substrate for HRP

			visualization on immunoblots
GeneJET PCR Purification Kit	Thermo Scientific	K0701	Purification of PCR products
GeneJET Plasmid MiniPrep Kit	Thermo Scientific	K0503	Isolation of plasmid DNA in *E. coli*
Promega Wizard® SV Gel and PCR Clean-Up System	Promega	A9280/A9281/ A9282/A9285	Purification of PCR products and gel-eluted DNA fragments
QIAquick® Gel Extraction Kit	QIAGEN	28706	Purification of gel-eluted DNA fragments
Wizard® Plus SV Minipreps DNA Purification System	Promega	A1460	Isolation of plasmid DNA in *E. coli*

2.1.10. Antibodies

Primary Antibody	**Target protein**	**Dilution**	**Source**
α-E (from rabbit)	Major capsid protein E of ΦCh1	1:2500	Klein *et al*., 2000
α-M.*Nma*φCh1I (from rabbit)	ΦCh1 main DNA methyltransferase	1:2500	Till, 2011
α-gp44 (from mouse)	ΦCh1 gp44	1:500	Iro, 2006
Secondary Antibody			
ECL™ Anti-Rabbit IgG, HRP linked whole antibody from donkey	Rabbit Immunoglobulin G	1:5000	GE Healthcare Product Number: NA934
ECL™ Anti-Mouse IgG, HRP linked antibody from sheep	Mouse Immunoglobulin G	1:2500	GE Healthcare Product Number: NA931

2.1.11. Solutions and Buffers

2.1.11.1. *E. coli* – Competent cells

MOPS I

MOPS	100 mM
KCl	10 mM
RbCl	10 mM

pH 7.0 (adjusted with KOH)

MOPS II

MOPS	100 mM
KCl	10 mM
RbCl	10 mM

pH 6.2 (adjusted with KOH)

MOPS IIa

MOPS	100 mM
KCl	10 mM
RbCl	10 mM
Glycerol	15%

pH 6.2 (adjusted with KOH)

2.1.11.2. *N. magadii* – Competent cells and transformation reagents

Buffered high salt spheroplasting solution

NaCl	2 M
KCl	27 mM
Tris/HCl pH 8.0	50 mM

After autoclaving:
add 15% sterile filtered sucrose

Unbuffered high salt spheroplasting solution (UHSSS)

NaCl	2 M
KCl	27 mM

Buffered high salt spheroplasting solution with glycerol

NaCl	2 M
KCl	27 mM
Tris/HCl pH 9.5	50 mM
Glycerol	15%

After autoclaving:
add 15% sterile filtered sucrose

60% PEG 600

60% PEG 600
40% UHSSS

After autoclaving: add 15% sterile filtered sucrose

0.5 M EDTA	Proteinase K
0.5 M EDTA	Commercially available from
Autoclave	QIAGEN

2.1.11.3. DNA Methods

2.1.11.3.1. Gel electrophoresis

50x TAE		0.8% agarose
Tris/HCl pH 8.5 – 9	2 M	Agarose melted in 1x TAE
Acetic acid	1 M	
EDTA	100 mM	

5x DNA loading dye	
Xylene Cyanol	0.03%
Orange G	0.12%
Glycerol	96% w/v
Tris/HCl pH 8.0	20 mM
Autoclave	

2.1.11.4. Protein Methods

2.1.11.4.1. Polyacryamide gels and Western Blot

2x Laemmli buffer		5 mM sodium phosphate buffer	
SDS	2%	NaH_2PO_4	200 mM
β-mercaptoethanol	5%	Na_2HPO_4	200 mM
Glycerol	10%	pH 6.8	
Bromphenol blue	0.01%		

Tris/HCl pH 6.8	60 mM

30% acrylamide solution	
Acrylamide	29%
N, N'-methylenebisacrylamide	1%

10x SDS Running buffer	
Tris	250 mM
Glycine	1.92 M

Stacking gel buffer	
Tris/HCl pH 6.8	500 mM
SDS	0.4%
add ddH_2O to 250 ml	

Separating gel buffer	
Tris/HCl pH8.8	1.5 M
SDS	0.4%
add ddH_2O to 250 ml	

Coomassie staining solution	
Methanol	25%
Acetic acid	10%
Coomassie Brillant Blue R-250	0.15%

Coomassie destaining solution

10% acetic acid in ddH_2O

10x TBS	
Tris/HCl pH 8.0	250 mM
NaCl	1.37 M
KCl	27 mM

Transblot buffer	
Tris	48 mM
Glycine	39 mM
SDS	0.037%
Methanol	20%

Ponceau-S staining solution	
Ponceau-S	0.5%
Trichloracetic acid	3%

Blocking solution

5% milk powder in 1x TBS

Primary antibody	
BSA	0.3%
NaN_3	0.02%
Respectively diluted serum	
Spatula of *N. magadii* L13 acetone powder	

Secondary antibody

Respectively diluted secondary antibody in 1x TBS

2.1.11.4.2. Protein purification from *E. coli* under native conditions

Lysis buffer		Wash solution	
NaH_2PO_4	50 mM	NaH_2PO_4	50 mM
NaCl	300 mM	NaCl	300 mM
Imidazol	10 mM	Imidazol	20 mM
pH 8.0		pH 8.0	

Elution buffers

NaH_2PO_4	50 mM
NaCl	300 mM
Different imidazol concentrations:	120 mM, 250mM and 500 mM
pH 8.0	

2.1.11.4.3. Protein purification from *E. coli* under denaturing conditions

Buffer B (Lysis buffer)		Buffer C (Wash buffer)	
NaH_2PO_4	100 mM	NaH_2PO_4	100 mM
Tris	10 mM	Tris	10 mM
Urea	8 M	Urea	8 M
pH 8.0 (adjusted with NaOH before use)		pH 6.3 (adjusted with HCl before use)	

Buffer D (Elution buffer)		Buffer E (Elution buffer)	
NaH_2PO_4	100 mM	NaH_2PO_4	100 mM
Tris	10 mM	Tris	10 mM
Urea	8 M	Urea	8 M
pH 5.9 (adjusted with HCl before use)		pH 4.5 (adjusted with HCl before use)	

Renaturing buffer 1 (Dialysis)	
Urea	4 M
NaCl	2.5 M
Tris	50 mM
$MgCl_2$	5 mM
pH 8.0	

Renaturing buffer 2 (Dialysis)	
NaCl	4 M
Tris	50 mM
$MgCl_2$	5 mM
pH 8.0	

2.1.11.5. RNA methods

2.1.11.5.1. Denaturing urea PAGE

6% PAA	
Polyacrylamide	6%
Urea	8 M
in 1x TBE	

2x RNA loading dye	
Formamide	95%
SDS	0.02%
Bromphenol blue	0.02%
Xylene cyanol	0.01%
EDTA	0.5 mM

RNA elution buffer	
NaoAc pH 5.5	0.5 M
EDTA pH 8.0	1 mM
Autoclave	

96 % EtOH
stored at -20°C

70% EtOH
stored at -20°C

3 M NaoAc
3 M NaoAc in DEPC

2.1.11.5.2. mRNA interferase activity of gp44

2 mM EDTA
2mM EDTA in RNase-free water (DEPC)
Autoclave

5 M NaCl
5 M NaCl in DEPC
Autoclave

500 mM Tris

500 mM Tris/HCl in DEPC pH 8.0

2.2. Methods

2.2.1. DNA methods

2.2.1.1. Polymerase chain reaction (PCR)

Polymerase chain reaction (PCR) is a technique used to amplify DNA, where copies of a particular DNA sequence are generated. Different polymerases were used for the preparative and the analytical PCR.

2.2.1.1.1. PCR templates

Different templates were created depending on the experiment – most of which resulted from crude extracts of *E. coli* or *N. magadii*. 30 µl of culture were centrifuged for 3 minutes at 13.2 krpm at room temperature, the supernatant was subsequently discarded and the pellet was then resuspended in 100 µl sterile ddH_2O.
Purified φCh1 DNA, which was diluted 1:30 with sterile ddH_2O, was also used as a template.

2.2.1.1.2. Preparative PCR

For preparative PCRs, *Pfu* DNA polymerase was used, which is essential due to its remarkable thermo-stability. During amplification, *Pfu* is capable of incorporating 500 nucleotides per minute and it also contains a 3'-5' exonuclease activity, thus having the ability of proofreading. Consequently, *Pfu*-generated PCR fragments have

fewer errors than those generated by *Taq* DNA polymerase used for analytical PCR (see section 2.2.1.1.3.).

DreamTaq DNA polymerase has an increased sensitivity, as well as specificity, in comparison to the conventional *Taq* DNA polymerase. *DreamTaq*, on the other hand, is able to incorporate 1000 nucleotides per minute.

These two DNA polymerases used for preparative PCRs are excellent tools for cloning.

The general protocol for a preparative PCR was as follows:

Preparative PCR reaction

Component	**Volume in µl**
Template	1
5' Primer	5
3' Primer	5
2 mM dNTPs	10
10x *Pfu*/*DreamTaq* reaction buffer	10
ddH_2O	67
Pfu/*DreamTaq* polymerase	2
Total volume	100

Preparative PCR program

Step	**Time (min)**	**Temperature (°C)**	**Number of cycles**
Initial denaturation	4	94	1
Denaturation	1	94	35
Annealing	1	Tm**	
Elongation	t*	72	
Final elongation	2 x t	72	1

* t: calculated elongation time (*Pfu* – 500 bp/minute, *DreamTaq* – 1000 bp/minute)

** Tm: calculated annealing temperature (substracting 4°C of the primer with the lowest melting temperature.

2.2.1.1.3. Analytical PCR

Analytical PCRs were executed using *GoTaq*® DNA polymerase, which is able to amplify 1000 bp per minute. However, this polymerase lacks the 3'-5' exonuclease activity, therefore not having a proofreading activity, hence being able to amplify at a higher speed. The commercially available *GoTaq*® Green Master Mix does not only contain the polymerase itself, but also all the necessary PCR reagents without the template and the primers. This polymerase was used to search for positive transformants after cloning, therefore being referred to as "Test-PCR" accordingly.

The general protocol for an analytical PCR was as follows:

Analytical PCR reaction

Component	**Volume in µl**
Template	1.5
5' Primer	1.5
3' Primer	1.5
ddH_2O	8.5
GoTaq® Green Master Mix	12
Total volume	25

Analytical PCR program

Step	**Time (min)**	**Temperature (°C)**	**Number of cycles**
Initial denaturation	4	94	1
Denaturation	1	94	25
Annealing	1	Tm**	
Elongation	t*	72	
Final elongation	2 x t	72	1

* t: calculated elongation time (*GoTaq* – 1000 bp/minute)

** Tm: calculated annealing temperature (substracting 4°C of the primer with the lowest melting temperature.

2.2.1.1.4. Quality control of PCR product

The quality of the corresponding PCR products was controlled on a 0.8% agarose gel. 5 µl of the preparative PCR product was mixed with 5 µl 5x DNA loading dye, and applied onto the gel, whereas the analytical PCR product did not need to be mixed and supplemented with 5x DNA loading dye, due to the fact that the *GoTaq*® Green Master Mix already contained all the required reagents for loading and could therefore be directly loaded onto the gel.

2.2.1.2. Agarose gel electrophoresis

DNA fragments were separated by size using agarose electrophoresis. The prerequisite amount of agarose (depending on the size of the fragment – 0.8% agarose gel for fragments above 700 bp) was dissolved in 1x TAE buffer, melted and then poured into the tray.
As previously mentioned, preparative PCR products were mixed with 5x DNA loading dye prior loading. The appropriate power ranged between 100-170 V. After the DNA separation, the gel was subsequently stained in an ethidium bromide (EtBr) bath (800 µl EtBr in 800 ml ddH_2O) and then shortly rinsed. The separated DNA fragments were thereafter visualized via UV light.

2.2.1.3. 6% Polyacrylamide gel electrophoresis

DNA fragments smaller than 700 bp were separated using a 6% polyacrylamide gel (PAA) in 1x TBE buffer. The DNA samples were prepared the exact same way as described above (see section 2.2.1.1.4.). Here, the applied power was 100 V. After the DNA separation, the gel was stained in an EtBr bath, rinsed and then visualized via UV light.

2.2.1.4. Purification of DNA

2.2.1.4.1. Purification of PCR products

PCR products were purified using the "GeneJET PCR Purification Kit" from Thermo Scientific or the "Promega Wizard® SV Gel and PCR Clean-Up System" from Promega. Purification was mandatory, as to get rid of the nonessential residues of the PCR reagents. The purified PCR products were then eluted in 50 µl ddH_2O.

2.2.1.4.2. DNA gel elution and purification

Gel elution was necessary and was therefore performed as to remove amplification errors during PCR. The DNA fragment was restricted and separated on a 0.8% agarose gel. UV light (70% UV light intensity to keep DNA damage as low as possible) was hereby used to visualize the DNA fragment of interest, which was then excised from the agarose gel. Purification was done following the protocol from QIAquick® Gel Extraction Kit. The DNA fragment was then eluted in 50 µl ddH_2O, and its concentration was measured by a spectrophotometer NanoDrop™ ND-2000c from Thermo Scientific.

2.2.1.5. DNA restriction

All restrictions were performed using restriction enzymes from Thermo Scientific. Reaction buffers were selected upon the manufacturer's recommendation, and the incubation time was performed either for 3 hours or overnight at 37°C. The completion of the restriction was analyzed on a 0.8% agarose gel, with the unrestricted plasmid as a negative control.

DNA restriction reaction

Component	Volume in µl
DNA	30
Restriction enzyme	2
10x Restriction buffer	5
ddH_2O	11
Total volume	50

2.2.1.6. DNA ligation

To perform cloning, both DNA fragment of interest and the desired plasmid, which were restricted with the same enzymes, were ligated using T4-DNA Ligase from Promega. The incubation time for ligation was done either for 3 hours at room temperature or overnight at 4°C.

Ligation mixture

Component	Volume in µl
Restricted DNA fragment	11.5
Restricted plasmid	1
10x T4 Ligase buffer	1.5
T4-DNA ligase	1
Total volume	15

2.2.2. Transformation in *E. coli*

2.2.2.1. Generation of competent *E. coli* cells

The preparation of competent *E. coli* cells (XL1-Blue, Lemo 21(DE3)) was achieved as follows: the strain of choice was inoculated in 200 ml of LB medium supplemented

with the respective antibiotics for selection (and 1 mM L-rhamnose for Lemo21(DE3)) to an OD_{600} of 0.1. The culture was incubated at 37°C, shaking at 165 rpm, until it has reached an OD_{600} of 0.6. The cells were then harvested by centrifugation at 10 krpm for 10 minutes at 4°C and the supernatant was thereafter discarded. The pellet was subsequently resuspended in 80 ml MOPS I and incubated on ice for 10 minutes. A second centrifugation step at 10 krpm for 10 minutes at 4°C followed, and the supernatant was again removed. The resulting pellet was resuspended in 80 ml MOPS II and incubated on ice for 30 minutes. The last centrifugation step was carried out at 10 krpm for 10 minutes at 4°C. Again, the supernatant was discarded, whereas the pellet was resuspended in 4 ml MOPS IIA. 100 µl aliquots of the generated competent cells were transferred into sterile Eppendorf tubes and eventually stored at -80°C until final use.

2.2.2.2. Transformation of competent *E. coli* cells

The protocol for the transformation of the strains XL1-Blue and Lemo21 (DE3) was performed the same way. Here, a 100 µl aliquot of the competent cells stored at -80°C was thawed on ice for 10 minutes. The ligation mixture (15 µl) was added to the competent cells accordingly, and then incubated on ice for 30 minutes. A subsequent heat shock at 42°C for 2 minutes was necessary for a successful transformation, which was then followed by a short incubation on ice. For regeneration, 300 µl LB medium was added and the cells were thereafter incubated at 37°C without shaking for 30 minutes. Finally, 100 µl of the transformation batch was plated on LB agar plates with the required antibiotics and incubated at 37°C overnight.

2.2.2.3. Screening of *E. coli* transformants

2.2.2.3.1. Quick-Prep

Quick-Prep is a method that was used as a preliminary screening for positive transformants, wherein the visible single colonies from the transformation LB agar

plates were inoculated into test tubes with 5 ml LB containing the required antibiotics for selection and then incubated at 37°C, shaking at 165 rpm, overnight.
300 µl of the culture deriving from a single colony was centrifuged at 13 krpm for 3 minutes at room temperature. The supernatant was discarded and the pellet was resuspended in 30 µl 5x DNA loading dye and then vortexed well. Adding 14 µl of 1:1 Phenol/Chloroform then followed and subsequently vortexed for 30 seconds. After vortexing, the samples were centrifuged at 13 krpm for 5 minutes at room temperature. Soon after, 12 µl of the supernatant containing the chromosomal DNA, plasmid DNA and RNA were loaded on 0.8% agarose gel. A negative control with the empty plasmid was also essential to have a better comparison to the putative positive clone, and therefore was also loaded on the 0.8% agarose gel. After visualization, the putative positive clones were identified considering the difference in separation behavior of plasmids with different size. The plasmids of the putative positive clones were larger in size than the empty plasmid (negative control).
Consequently, the plasmids of the putative positive clones were isolated using the GeneJET Plasmid MiniPrep Kit from Thermo Scientific or the Wizard® Plus SV Minipreps DNA Purification System from Promega and analyzed by analytical PCR and/or test restriction.

2.2.2.3.2. Analytical PCR

Analytical PCR was a useful tool to search for the positive transformants as mentioned in section 2.2.1.1.3. For this screening, *Taq* DNA polymerase was used to test if the plasmids of the putative positive clones contain the DNA fragment of interest, thus yielding a positive PCR signal.
After the verification of the positive transformant, 100 µl of the positive clone was inoculated into 20 ml LB medium with the required antibiotics and incubated at 37°C, shaking at 165 rpm, overnight, to obtain a fresh culture. 800 µl of 50% glycerol was then added to 1 ml of the fresh overnight culture and then stored at -80°C.

2.2.2.3.3. Test restriction analysis

Another screening method for positive transformants is the test restriction analysis, wherein the plasmid DNA of a putative positive clone was restricted with the same restriction enzymes that were previously used to restrict the empty plasmid. In doing so, in case of a positive clone, the inserted DNA fragment could be restricted from the plasmid and eventually visualized on a 0.8% agarose gel.

After these screening methods, final confirmation of the positive transfromant was performed by sequencing the plasmid DNA through Microsynth AG.

2.2.3. Transformation in *N. magadii*

2.2.3.1. Preparation of competent *N. magadii* cells

To prepare competent *N. magadii* cells, three 500 ml baffled-bottom Erlenmeyer flasks with 60 ml NVM^+ rich medium were inoculated with freshly grown culture of *N. magadii*. These three flasks were inoculated with a different, increasing volume of *N. magadii*: 2 ml, 4 ml and 6 ml. Bacitracin with a final concentration of 70 µg/ml was also added to the NVM^+ rich medium. The cells were subsequently grown at 37°C, shaking at 165 rpm, until one of the three cultures reached an OD_{600} of 0.5 to 0.6. The cells were then harvested by centrifugation at 6 krpm for 15 minutes at room temperature, the supernatant discarded and the resulting pellet resuspended in half of the volume buffered high salt spheroplasting solution with glycerol. The cell suspension was subsequently transferred into a 100 ml Erlenmeyer flask and Proteinase K was then added to a final concentration of 0.1%, which enables disgestion of the S-layer. The cells were thereafter incubated at 42°C, shaking at 150 rpm, for approximately 48 hours until they became spheroplasts, which could be visualized via microscope analysis.
As soon as the spheroplasts became visible, 1.5 ml aliquots of the competent *N. magadii* cells were prepared. These competent cells were either used immediately for transformation or stored at -80°C for one week.

2.2.3.2. Transformation of competent *N. magadii* cells

1.5 ml of the competent *N. magadii* cells were thawed and centrifuged at 10 krpm for 3 minutes at room temperature. The supernatant was discarded and the resulting pellet resuspended in 150 µl high salt spheroplast solution without glycerol. 15 µl of 0.5 M EDTA pH 8.0 was then added and incubated at room temperature for 10 minutes. Subsequently, plasmid DNA (3-5 µg/10 µl DNA or 20-50 µg/10 µl DNA for deletion mutants) was added to transform into the competent cells. 10 µl is the maximum volume that could be added, as to ensure that the NaCl concentration stayed constant for the transformation. The cells were then incubated at room temperature for 5 minutes. Thereafter, 150 µl of 60% PEG 600 in high salt unbuffered spheroplasting solution were added and then incubated at room temperature for 30 minutes. 1 ml NVM^+ rich medium was then added and the transformation batch was centrifuged at 10 krpm for 5 minutes at room temperature. To wash off the residual PEG-600, the resulting pellet was resuspended in 1 ml NVM^+ and centrifuged again at 10 krpm for 5 minutes at room temperature. The cells were subsequently incubated at 37°C, shaking at 165 rpm, until the cells had regenerated and had regained their rod-shaped structure. It was necessary to change to medium every day, in order for the cells to have fresh medium whilst regenerating. This was done by centrifugation at 10 krpm for 5 minutes at room temperature. The cells were also analyzed via microscope every day to see if they had regained their S-layer, thus having a rod-shaped structure.
As soon as more than 90% of the cells had regenerated, they were plated on NVM^+ rich medium agar plates with the required antibiotics (100 µl per plate) and then incubated at 42°C in sealed plastic bags for approximately two to three weeks until colonies were visible.

2.2.3.3. Screening of *N. magadii* transformants

As soon as colonies were visible, single colonies were inoculated in 500 µl NVM^+ rich medium in Eppendorf tubes and then incubated at 37°C, shaking at 165 rpm, for a few days until the cultures have grown. To ensure better growth of *N. magadii*, the Eppendorf tubes were opened for approximately 2 minutes, as to aerate the cultures,

since *N. magadii* is strictly aerobic. Templates were then prepared as previously described in section 2.2.1.1.1. and tested via analytical PCR (see section 2.2.1.1.3.).

2.2.4. Protein methods

2.2.4.1. Preparation of protein crude extracts

The production of the protein of interest from *E. coli* and *N. magadii* was detected via SDS-PAGE and Western Blot. Prior to these, it was necessary to prepare crude protein extracts, wherein 1.5 ml of cell culture was centrifuged at 13 krpm for 3 minutes at room temperature. The supernatant was discarded and the resulting pellet was resuspended in x µl 5 mM sodium phosphate buffer pH 6.8 and x µl 2x Lämmli buffer (x = OD_{600} x 75). The sample was denatured at 95°C for 10 minutes before it was loaded on a SDS-PAGE gel or stored at -20°C.
As for *N. magadii* crude protein extracts, it was essential to incubate the samples at 37°C overnight until the sample was not viscous anymore, before denaturing the protein samples at 95°C for 10 minutes.

2.2.4.2. SDS-PAGE

The separation of proteins according to their molecular weight was performed via SDS-PAGE (sodium dodecyl sulphate polyacrylamide gel electrophoresis). Proteins are denatured by the anionic detergent SDS, which disrupts the tertiary structure of the proteins and coats their intrinsic charge, thus giving the proteins a negative charge. The discontinuous polyacrylamide gel was prepared using the equipment from BioRad-Mini-PROTEAN.

Composition of an SDS-PAGE gel

Component	12% Separating gel	4% Stacking gel
30% Polyacrylamide	2 ml	267 µl
Separating gel buffer	1.25 ml	-
Stacking gel buffer	-	500 µl
ddH_2O	1.75 ml	1.233 ml
Total volume	5 ml	2 ml
Mixed on ice		
10% APS	60 µl	20 µl
TEMED	10 µl	5 µl

The 12% PAA separating gel was initially poured and was coated with isopropanol without delay, as to avoid air bubbles. After polymerization of the separating gel, the isopropanol was removed and the 4% PAA stacking gel mixture was prepared, which was eventually poured on top of the separating gel. A 10-well comb was inserted carefully between the glass plates. After the polymerization of the stacking gel, the SDS-PAGE gel was assembled with the electrode and the buffer tank as well as the chamber was filled with 1x SDS-PAGE buffer. The comb was then gently removed and the protein samples were loaded onto the gel. A pre-stained protein marker was also loaded onto the gel, in order to visualize the size of the proteins.

For *E. coli* protein samples, gel electrophoresis was started with 40 V to accumulate the protein samples into the pockets. The voltage was then increased to 60 V until the bromphenol blue had reached the border of the stacking and the separating gels. As soon as the bromphenol blue had reached the separation gel, the voltage was increased at 100 V.

In contrary, *N. magadii* protein samples were separated continuously with only 40 V due to their high salt concentration.

2.2.4.3. Coomassie staining

To visualize the protein concentration after separation, Coomassie staining was performed. The separating gel containing the separated proteins was detached from the stacking gel and stained for approximately 5-15 minutes in Coomassie staining solution. The staining solution was removed and the gel was then incubated with destaining solution until clear protein bands with a clear background were visible. The protein concentration could herewith be determined.

2.2.4.4. Western Blot

The method used to detect and determine specific proteins in a sample is the Western Blot, also called the protein immunoblot. This technique consists of three main steps, in which (1) the proteins are separated by size via SDS-PAGE (see section 2.2.4.2.), (2) then transferred onto a nitrocellulose membrane and (3) eventually visualized via exposure to specific primary and secondary antibodies. The specific primary antibody is directed against the target protein, wherein the secondary antibody is directed against the primary antibody. The secondary antibody is combined with a reporter enzyme horseradish peroxiase (HRP), which produces luminescence in the same ratio as the protein concentration.

2.2.4.4.1. Transfer of the proteins via semi-dry blotting system

After the separation of proteins by size via SDS-PAGE (see section 2.2.4.2.), the proteins were transferred onto a nitrocellulose membrane by using an electric field, enabling the proteins to move from the SDS-PAGE gel onto the membrane. For this step, three Whatman filter papers (9 x 6 cm) were incubated in transfer buffer one by one and put on the blotting device Trans-Blot® Turbo™ Transfer System from BioRad. Afterwards, the nitrocellulose membrane (9 x 6 cm; GE Healthcare Amersham™ Protran™ 0.2 µm NC) was also incubated in transfer buffer and put above the first three Whatman filter papers. The SDS-PAGE gel containing the

separated proteins was incubated in ddH_2O for 5 minutes, then shortly incubated in transfer buffer, and eventually carefully put on top of the nitrocellulose membrane. To protect and cover the SDS-PAGE gel, a layer of three Whatman filter papers, which have also been incubated in transfer buffer, was used. A rolling device was used to remove the air bubbles in between the layers, to ensure good blotting results.

The pre-installed blotting protocol from Bio Rad was herewith applied for one or two mini gels: 25 mA for 30 minutes.

2.2.4.4.2. Ponceau S staining

After blotting, the membrane was stained for approximately 5 minutes with Ponceau S staining solution, which is a red dye that enables the detection of proteins. This could be easily destained with tap water.

2.2.4.4.3. Blocking of the membrane

After destaining the blot with tap water, the nitrocellulose membrane was incubated in 5% milk powder in 1x TBS at 4°C, gently shaking overnight to prevent unspecific binding of the antibodies to the membrane.

2.2.4.4.4. Incubation with antibodies

After blocking, the nitrocellulose membrane was rinsed with 1x TBS until there were no remains of the blocking solution anymore. α-E antibody as well as the α-M.*Nma*φCh1I antibody was diluted to a final 1:2500 dilution, whereas the α-gp44 antibody was diluted to a final 1:500 dilution. The primary antibody solution was complemented to a final concentration of 0.3% BSA and 0.02% NaN_3. Furthermore, one spatula of acetone powder from *N. magadii* L13 was added, in order to saturate the antibodies. 10 ml of the primary antibody solution was applied onto the membrane

and incubated for one hour whilst gently shaking to evenly distribute the antibody on the gel. The primary antibody solution may be reused and was therefore collected and stored at 4°C. Afterwards, the membrane was washed three times with approximately 100 ml 1x TBS for 10 minutes for each washing step and eventually incubated with 10 ml freshly prepared secondary antibody for an hour while gently shaking. The secondary antibodies that were used here were: α-rabbit (1:5000 final dilution in 1x TBS) and α-mouse (1:2500 final dilution in 1x TBS). Subsequently, the secondary antibody solution was discarded and the nitrocellulose membrane was again washed three times with 1x TBS as previously done.

2.2.4.4.5. Detection

Detection was achieved using the Clarity^{TM} Western ECL Substrate Kit from BioRad. The horseradish peroxidase that was coupled with the secondary antibody was herewith detected by oxidzing its enhanced chemiluminiscent (ECL) substrate luminol, whilst emitting light. 1 ml of each substrate from the detection kit (HRP substrate peroxide solution and HRP substrate luminol reagent) were pipetted onto the membrane and incubated for 5 minutes, whilst occasional shaking as to ensure an even distribution of the substrates. The blot was then detected using the ImageLab program and the exposure time varied from 10-240 seconds.

2.2.4.5. Protein purification (gp44) from *E. coli* under native conditions

Lemo21(D3) carrying pREP4-pRSET-A-ORF44 was inoculated in 500 ml LB medium with ampicillin, chloramphenicol and kanamycin and incubated at 37°C, shaking at 165 rpm, overnight. The culture was then inoculated in 5 l LB medium with 1 mM L-rhamnose to an OD_{600} of 0.1 and was grown at 37°C, shaking at 165 rpm, to an OD_{600} of 0.3. Here, a protein sample was prepared as described in section 2.2.4.1. and was eventually loaded on an SDS-PAGE gel. Subsequently, the culture was induced with 0.4 mM IPTG and further grown at 28°C, shaking at 165 rpm, for 4

hours until the cells were harvested. After induction and incubation at 28°C, another protein sample was prepared for the SDS-PAGE. The culture was centrifuged at 6 krpm at 4°C for 15 minutes, the supernatant was discarded and the pellet was frozen at -80°C overnight. Resuspension of the pellet in 350 ml lysis buffer after thawing on ice (see section 2.1.11.4.2.) then followed the next day. Afterwards, the cell suspension was sonicated under constant cooling with ice for approximately 3x 5 minutes until the cells were adequately lysed, which was observed via microscope. Another centrifugation at 10 000 g at 4°C for 20 minutes then followed, as to remove the cell debris and insoluble proteins. 1.5 ml of Nickel Agarose (Ni-NTA) slurry from QIAgen were added to the supernatant and stirred overnight at 4°C. Ni-NTA agarose enabled the His-tagged gp44 to bind to the Ni^{2+} ions via affinity chromatography. The lysate-resin mixture was loaded onto a column and the flow-through was collected. The Ni-NTA bound with the protein was left in the column and washed twice with 4 ml washing buffer. Elution with 4 x 500 µl of each elution buffers (different elutions were achieved by raising the imidazole concentration). From each fraction (flow-through up to the last elution), protein samples were taken and loaded onto an SDS-PAGE gel along with the two other protein samples that had previously been taken (before and after induction) to enable analysis of the protein purification.

2.2.4.6. Protein purification (gp44) from *E. coli* under denaturing conditions

2.2.4.6.1. Denaturing conditions

Gp44 purified under denaturing conditions was prepared and collected as described in section 2.2.4.5. However, the overnight culture was inoculated in 2 l LB with 1 mM L-rhamnose to an OD_{600} of 0.1.

After thawing the cell pellet on ice, it was resuspended in 180 ml Buffer B (see section 2.1.11.4.3.), a spatula tip full of egg white lysozyme was added and the suspension stirred at room temperature overnight. Subsequently, the suspension was sonicated as per section 2.1.11.4.5. After centrifugation at 10 000 g at 4°C for 20

minutes, 700 µl Ni-NTA slurry was added to the supernatant and stirred overnight at room temperature. The suspension was then loaded onto a column and the flow-through was collected. The Ni-NTA bound with the protein was left in the column and washed twice with 6 ml Buffer C. Elution with 4 x 500 µl Buffer D and then 4 x 500 µl Buffer E was then carried out. From each fraction (flow-through up to the last elution), protein samples were taken and loaded onto an SDS-PAGE gel along with the two other protein samples that had previously been taken (before and after induction) to enable analysis of the protein purification.

2.2.4.6.2. Protein renaturation by dialysis

Purified gp44 was transferred into dialysis tubes and dialyzed against renaturing buffer 1 (see section 2.1.11.4.3.) containing 4 M urea for an hour. Overnight dialysis with a fresh renaturing buffer 1 was then performed. Subsequently a second dialysis step against renaturing buffer 2 was carried out for an hour, and here again, the buffer was then changed with a fresher one and the dialysis with renaturing buffer 2 continued overnight. The protein solution was collected and transferred into Eppendorf tubes. It was then centrifuged at 13 krpm for 3 minutes at room temperature to eliminate the residual insoluble protein. Samples from the protein solution were then taken and analyzed via SDS-PAGE (see section 2.2.4.2.) and Western Blot (see section 2.2.4.4.).

2.2.5. RNA methods

2.2.5.1. *In vitro* transcription

In vitro transcription of linearized pRSET-A-34 and pRSET-A-36 (restricted with *Hind*III) was achieved using the AmpliScribe™ T7-Flash™ Transcription Kit from Epicentre according to the manufacturer's protocol.

AmpliScribe T7-*Flash* Transcription Reaction

Component	Volume in µl
DEPC	x
Linearized template DNA with T7 promoter (1 µg)	x
AmpliScribe T7-*Flash* 10x Reaction Buffer + DTT	4
100 mM ATP	3.6
100 mM CTP	3.6
100 mM GTP	3.6
100 mM UTP	3.6
AmpliScribe T7-*Flash* Enzyme Solution	4
Total volume	40

The mixture was then incubated at 37°C for 3 hours and stored at -80°C.

2.2.5.2. Denaturing urea PAGE

The quality and quantity controls of RNA fragments were analyzed using a 6% polyacrylamide gel (PAA) in 1x TBE buffer and 8 M urea. To dissolve the 8 M urea, it was necessary to pre-heat the 1x TBE buffer due to the fact that urea is endothermic and is therefore difficult to dissolve without any precipitation. 10% APS and TEMED were only added into the solution when it had been cooled down at room temperature and was subsequently poured onto the gel-casting module. A 10-well comb was inserted carefully between the glass plates. After the polymerization of the denaturing urea polyacrylamide gel, it was assembled with the electrode and the buffer tank as well as the chamber was filled with 1x TBE buffer. The comb was then gently removed. It was necessary to pre-run the urea PAGE before loading the RNA samples to equilibrate the gel and also to remove urea from the wells by manually rinsing them

out of the wells prior sample loading to ensure proper bands. 4 µl of 2x RNA loading dye were added onto 2 µl of RNA sample. This mixture was then incubated at 65°C for 3 minutes to get rid of the secondary structures of the RNA and then eventually loaded onto the gel alongside the RNA ladder. The applied power was 20 mA until the xylene cyanol was almost at the bottom of the gel. After the DNA separation, the gel was stained in an EtBr bath, rinsed and then visualized via UV light.

2.2.5.3. RNA gel elution and purification

Gel elution was necessary and was therefore performed as to remove unwanted RNA bands. The entire RNA mixture was loaded and separated on a denaturing urea polyacrylamide gel in order to purify the RNA of interest. The sample was prepared and the gel was run in accordance to the previously described protocol (see section 2.2.5.2.). After the separation, the lane with the RNA marker and a small section of the lanes with the RNA were excised out of the gel, stained in an EtBr bath and visualized by UV light. It was necessary to stain only a small part of the separated RNA to see if the separation had worked and to use as a template for gel elution. It was important not to stain all of the separated RNA, as to prevent contamination with EtBr. The stained gel was marked and the RNA of interest was cut out of the gel, serving as a template. The template was then put beside the unstained gel to show where the remaining RNA of interest (unstained) was, which was then excised out of the gel and put into an Eppendorf tube. 800 µl of the RNA elution buffer and 40 µl of phenol (specifically for RNA) were then added into the Eppendorf tube containing the gel with the RNA of interest. Subsequently, the mixture was then incubated at 4°C overnight. On the next day, it was incubated at 37°C, shaking at 1.3 krpm, for 4 hours to remove the RNA out of the gel. Afterwards, the supernatant was divided (approximately 400 µl each) and transferred into two new Eppendorf tubes. 200 µl phenol and 200 µl chloroform were then added to each of the tubes, which were then vortexed well. Centrifugation at 13.2 krpm for 3 minutes at room temperature then followed, allowing the supernatants to be collected into new Eppendorf tubes. The supernatants were then washed with 400 µl chloroform each, shaked and then centrifuged at 13.2 krpm for 3 minutes at room temperature. The resulting aqueous

phases were then transferred into new Eppendorf tubes, and 40 µl 3 M NaoAc and 1 ml 96% EtOH were added into each of the tubes. These were then stored at -20°C overnight, wherein the precipitation of the RNAs took place.

After the overnight precipitation, a centrifugation step at 14 krpm at 4°C for 40 minutes then followed. The supernatants were discarded, the resulting pellets were each washed with 200 µl 70% EtOH and then centrifuged at 14 krpm at 4°C for 10 minutes. The supernatants were removed and the pellets were dried at room temperature by leaving the lids of the Eppendorf tubes open for approximately 15 minutes. The pellets were then resuspended in 10-20 µl DEPC and stored at -20°C. The concentration of the RNAs was also measured by NanoDrop™ ND-2000c from Thermo Scientific.

2.2.5.4. mRNA interferase activity of gp44

Purified gp44 was incubated with the RNAs of interest (ORF34-3' and ORF36-3') at 37°C for 30 minutes. The reaction mixtures consisted of different NaCl concentrations to investigate in which NaCl concentration gp44 was more active.

Reaction mixtures

Component	**Volume in µl**
RNA	3
gp44 (0.006 µg/ µl)	5
0.1 mM EDTA	1 (Stock: 2 mM)
NaCl*	x
20 mM Tris pH 8	0.8 (Stock: 500 mM)
DEPC H_2O	x
Total volume	20

* 100 mM NaCl, 250 mM NaCl, 500 mM NaCl, 1 M NaCl and 2.5 M NaCl

After the incubation at 37°C, the reaction was analyzed via denaturing urea PAGE to see if there were any changes in the RNA.

2.2.6. Cell culture passaging

2.2.6.1. Stability of *N. magadii* L11-ΔORF44 deletion mutant

To analyze the stability of *N. magadii* L11-ΔORF44 deletion mutant, cell culture passaging was performed (see Figure 12). The wild type *N. magadii* L11 was also passaged in order to have a direct stability comparison to the mutant strain. Plaques from virus titers of both *N. magadii* L11 and *N. magadii* L11-ΔORF44 were each inoculated into 10 ml NVM^+ rich medium. The deletion mutant was always inoculated in NVM^+ rich medium with and without the selective antibiotic *novobiocin*. The cultures were then grown at 42°C, shaking at 150 rpm.

Afterwards, the pre-cultures were produced as follows: The cultures were inoculated into 20 ml NVM^+ rich medium (+ *novobiocin*) to an OD_{600} of 0.1 and incubated at 37°C, shaking at 165 rpm for 72 hours.

The pre-cultures were then inoculated into 40 ml NVM^+ (+ *novobiocin*) to an OD_{600} of 0.1 (day 0) and incubated at 37°C, shaking at 165 rpm, until day 7. The OD_{600} was measured every day (day 1 to day 7). After onset of lysis, the cultures were re-inoculated to an OD_{600} of 0.1 into 20 ml NVM^+ (+ *novobiocin*), thus generating new pre-cultures, which were then grown and re-inoculated for the following seven passages. 1.5 ml samples were also taken after onset of lysis, centrifuged at 13.2 krpm for 3 minutes at room temperature and the pellet was resuspended into x µl ddH_2O depending on the OD_{600} (OD_{600} 1.000 = 100 µl ddH_2O added). A 1:10 dilution of the cell suspensions was used for the templates used for analytical PCR.

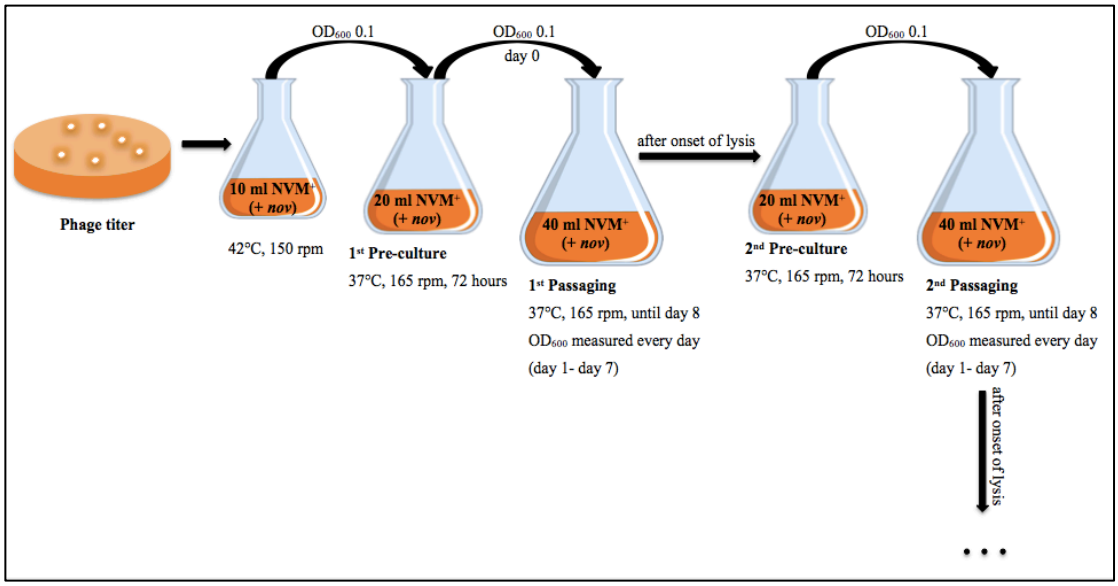

Figure 12. Cell culture passaging to analyze the stability of *N. magadii* L11-ΔORF44 in comparison to the wild type *N. magadii* L11.

A plaque from the virus titer was inoculated into 10 ml NVM^+ (+*nov*) and grown at 42°C. This culture was subsequently inoculated into 20 ml NVM^+ (+*nov*) to an OD_{600} of 0.1, grown for 72 hours at 37°C and generating the 1st pre-culture. It was then re-inoculated into 40 ml NVM^+ (+*nov*) to an OD_{600} of 0.1 (day 0), which represented the 1st passaging. This was incubated at 37°C until day 8. After onset of lysis, the 2nd pre-culture was generated and re-inoculated to passage the cell culture the second time. Pre-cultures were generated as soon as lysis began and the steps were repeated up to the 8th passaging.

2.2.6.2. Virus titers – appropriation by soft agar technique

Virus titer analysis was performed here to determine the concentration of φCh1 virus particles present in both the wild type *N. magadii* L11 and the *N. magadii* L11-ΔORF44 deletion mutant during all 8 cell culture passages. In order to do that, a growth curve analysis was performed and 1.5 ml samples were taken directly after onset of lysis at the same time in all passages. The samples were centrifuged at 13 krpm for 3 minutes at room temperature and 1 ml supernatant of every sample was complemented with 20 µl $CHCl_3$. Dilution series of the supernatants (with NVM^+) were prepared: 10^{-2}, 10^{-4}, 10^{-6}, 10^{-8}, 10^{-10}. 300 µl of *N. magadii* L13, which was grown to late log or stationary phase, and 100 µl of each dilution were added to 5 ml NVM^+ soft agar (heated at 55°C to maintain its liquid state). The mixture was shortly

vortexed and poured onto non-selective NVM^+ rich medium plates. The plates were then incubated at 37°C in tightly sealed plastic bags for about a week until virus plaques became visible. As soon as plaques were visible, they were counted and the plaque-forming units per ml (pfu/ml) were calculated.

2.2.7. Cloning strategies

2.2.7.1. pNB102-ORF94-M2

In order to create a mutation in the upstream region of M.*Nma*φCh1I, PCR was performed using φCh1 template and primers MT-Xba-3 and MT-M-Kpn that yielded a length of approximately 1253 bp. The DNA polymerase that was used was *Pfu*. The PCR fragments were then restricted with *Xba*I and *Kpn*I and subsequently ligated into pNB102, which had previously been restricted with the same restriction enzymes. The constructed plasmid was then named pNB102-ORF94-M2 and was transformed into *N. magadii* L13.

2.2.7.2. pNB102-p43-44

In order to complement the φCh1 ORF44 deletion mutant, it was necessary to place the ORF44 alongside with the promoter p43, which is shared by the φCh1 ORF43, into the shuttle vector pNB102. The fragment p43-44 was amplified via PCR by using pRo-p43-44 as a template and primers 43-Kpn-5 and 44-3-Xba that yielded a length of about 877 bp. The DNA polymerase that was used was *DreamTaq*. The PCR fragments were then restricted with *Xba*I and *Kpn*I as well as the plasmid pNB102. The restricted fragments and the restricted pNB102 were then ligated and the construct was then named pNB102-p43-44.

2.2.7.3. pRSET-A-34

ORF34 was amplified using the primers 34-3 and 34-D-5 and the φCh1 template that yielded around 540 bp. The DNA polymerase that was used was *DreamTaq*. The fragment was restricted with *Bgl*II and *Hind*III and was ligated into the plasmid pRSET-A that was restricted with *Bam*HI and *Hind*III. The construct was thereafter named pRSETA-34 and was transformed into XL1-Blue.

2.2.7.4. pRSET-A-36

ORF36 was amplified using the primers 36-3 and 36-D-5 and the φCh1 template that yielded around 600 bp. The DNA polymerase that was used was *DreamTaq*. The fragment was restricted with *Bam*HI and *Hind*III and was ligated into the plasmid pRSET-A that was restricted with the same restriction enzymes. The construct was thereafter named pRSETA-36 and was transformed into XL1-Blue.

3. Results and Discussion

3.1. Results

3.1.1. Stability of the ΦCh1 ORF44 deletion mutant

ΦCh1 ORF44 is a 395 bp open-reading frame upstream of the ΦCh1 DNA replication domain (Klein *et al*., 2002). In 2017, Yan Gillen constructed and carried out introductory studies on the ΦCh1 ORF44 deletion mutant, wherein preliminary outgrowth experiments were performed. The growth and lysis behavior of the wild type strain *N. magadii* L11 was compared to that of *N. magadii* L11-ΔORF44. It was demonstrated that ORF44 influences the onset of lysis, as it occurred 24 hours earlier in *N. magadii* L11-ΔORF44 in comparison to that of the wild type *N. magadii* L11. Lysis kinetics as well as virus titer experiments, however, concluded that there was no significant difference in the amount of released viral particles during lysis when comparing both strains. Gillen came upon two other observations, one of which was the fact that grown cultures of *N. magadii* L11-ΔORF44 spontaneously lysed after a few days of staying on the bench without being incubated at either 37°C or 42°C. Furthermore, sub-culturing an N. magadii L11-ΔORF44 culture to three to four passages led to a growth behavior comparable to the cured strain *N. magadii* L13, thus no longer exhibiting lysis after three to four passages as opposed to the wild type *N. magadii* L11 (data not shown). This demonstrates that passage number affects the characteristics of these strains.

3.1.1.1. Aim

The aim of this study was to investigate the stability of strain *N. magadii* L11-ΔORF44 culture after eight cell culture passages. The exact same handling of each culture was necessary to eliminate variables. This was achieved as described in 'Material and Methods' by passaging both the wild type *N. magadii* L11 and the mutant strain to have a direct stability comparison (see section 2.2.6.1.). Their growth and lysis behaviors, as well as the quantity and quality of the virus particles released after onset of lysis, were analyzed.

3.1.1.2. Cell culture passages

Figure 13 illustrates the different growth kinetics of *N. magadii* L11 in comparison to *N. magadii* L11-ΔORF44 during the first five passages. Therefore, the cultures were incubated in rich medium at 37°C with agitation. Growth and lysis of the cultures were monitored by measuring the optical density at 600 nm (OD_{600}) over a time period of 7 days. After 3 days, the cultures were used to inoculate fresh medium to start the next passage. As evident on the graphs, *N. magadii* L11-ΔORF44 lysed 24 hours prior the wild type *N. magadii* L11 during the 1st passage. As for the 2nd passage, the mutant strain started lysing much weaker than before (1st passage). From the 3rd passage onwards, however, *N. magadii* L11-ΔORF44 did no longer show an optical lysis – it seemed as if the culture stayed in the stationary growth phase. On the contrary, lysis could still be observed for the wild type *N. magadii* L11 culture up to the 5th passage.

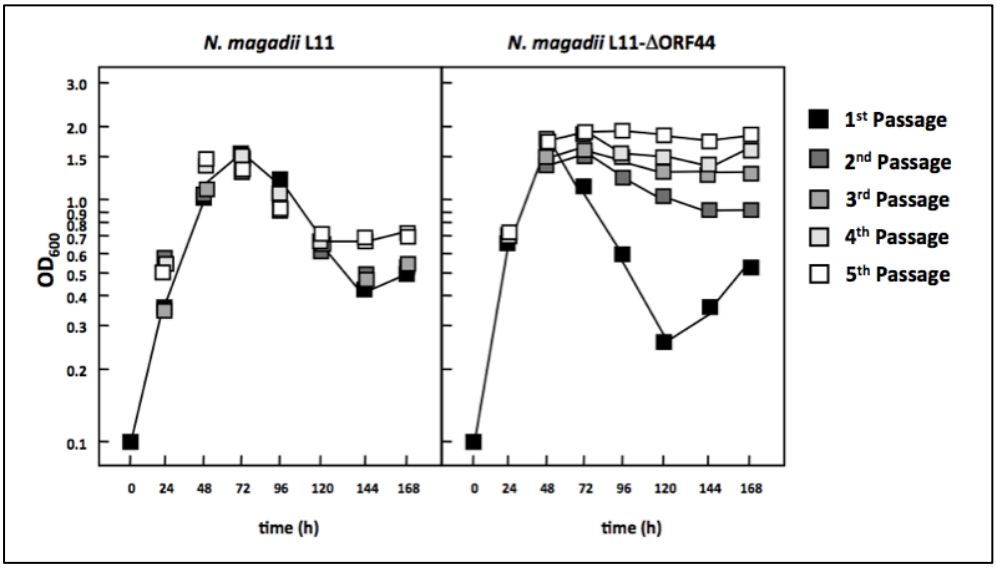

Figure 13. Growth kinetics analysis of the wild type *N. magadii* L11 vs. the mutant *N. magadii* L11-ΔORF44 during the first five cell culture passages.

Passages of cultures of the wild type *N. magadii* L11 and the mutant strain *N. magadii* L11-ΔORF44 were performed as described on section 2.2.6.1 and the optical density was measured at 600 nm. The 1st passage of *N. magadii* L11 and *N. magadii* L11-ΔORF44 shows differences in the onset of lysis, wherein the mutant strain started lysis 24 hours prior to the wild type. From the 3rd passage onwards, *N. magadii* L11-ΔORF44 no longer showed an optical lysis, whereas for the wild type, lysis could still be observed.

3.1.1.3. Qualitative assay of the viral infection

A preparative PCR was performed in order to verify if the wild type *N. magadii* L11 and the mutant *N. magadii* L11-ΔORF44 cultures were still infected with the virus, thus still containing the ΦCh1 genome. ORF56, a 540 bp open reading frame in the mid-section of the viral genome, was randomly chosen and amplified. As depicted on Figure 14, ORF56 could be detected in both strains from the 1st to the 5th passage, which concludes that they were still infected with the virus. This however, only shows the quality, but not the quantity of the viral infection.

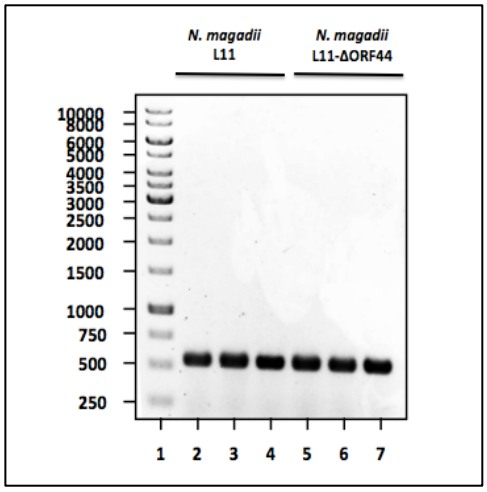

Figure 14. Qualitative viral infection in *N. magadii* L11 and *N. magadii* L11-ΔORF44

The preparative PCR was loaded on a 0.8% agarose gel to check for viral infection. ORF56 (approximately 540 bp) was amplified, thus confirming that both N. magadii L11 and N. magadii L11-ΔORF44 were still infected with ΦCh1 up until the 5th passage.

Lane 1: 1kb DNA Ladder
Lanes 2 and 5: 1st passage (wild type and mutant strain)
Lanes 3 and 6: 3rd passage (wild type and mutant strain)
Lanes 4 and 7: 5th passage (wild type and mutant strain)
On the left, the sizes of the DNA marker bands are indicated.

3.1.1.4. Virus titer analysis

In order to investigate the quantity of the virus particles released after onset of lysis (day 5 after inoculation of the strains) for the 1st up to the 5th passage, virus titer analysis was performed in accordance to the steps described on section 2.2.6.2. Figure 15 illustrates virus particle liberation of *N. magadii* L11 and *N. magadii* L11-ΔORF44. During the 1st passage of both strains, there is no significant difference in the amount of virus particles released. However, for *N. magadii* L11-ΔORF44, the virus titer assay shows that prolonged passage results in a crucial decrease in virus particle liberation. A decrease of about 4 to 5 magnitudes of order of the virus particles release could be determined comparing the 1st passage with the 5th passage.

With respect to the wild type *N. magadii* L11, there is no significant change in the amount of the released virus particles after onset of lysis throughout the five passages.

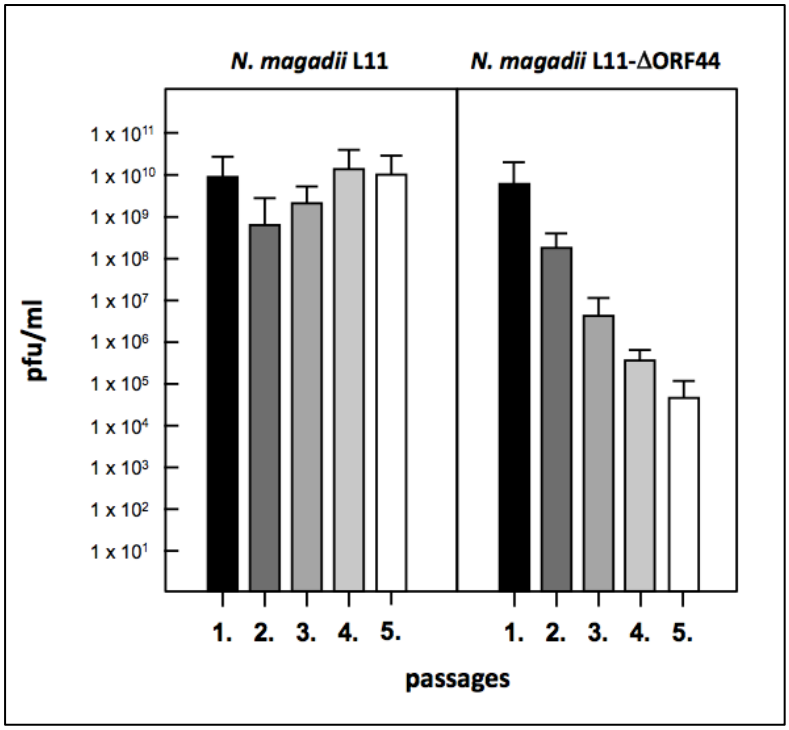

Figure 15. Virus titer analysis of *N. magadii* L11 and *N. magadii* L11-ΔORF44

Five days after inoculation of the cultures, samples were taken. Cells were separated from the supernatant by centrifugation. The supernatants were used to plate appropriate dilutions using top agar together with *N. magadii* L13 as an indicator strain. After 1 week of incubation at 37°C the virus titers were determined. The values of the virus titers (pfu/ml) are indicated as bars in black (1st passage), dark grey (2nd passage), middle grey (3rd passage), light grey (4th passage), and white (5th passage). Error bars are indicated, ± 1SD.

Virus titer analysis showed that there is no significant difference in the amount of phage particles released after the onset of lysis throughout the five passages of the *N. magadii* L11 culture. However, as evident on the graph for the *N. magadii* L11-ΔORF44 culture, the more passages it endured, the less amount of virus particles were liberated. An absolute decrease of the virus particle release of approximately 5 magnitudes can be seen from the 1st passage to the 5th passage.

3.1.1.5. Expression of ORF11 in *N. magadii* L11 and *N. magadii* L11-ΔORF44

The stability of *N. magadii* L11-ΔORF44 was further examined by investigating the expression of ORF11 encoding the major capsid protein E. Crude protein extracts of *N. magadii* L11 and *N. magadii* L11-ΔORF44 were prepared as described on section 2.2.4.1. The production of protein E was subsequently detected via Western Blot using α-E antibody (1:2500) (see section 2.2.4.).

As described in 'Material and Methods', protein samples were taken after onset of lysis in all passages. As shown on Figure 16, expression of the major capsid gene E could be detected in all five passages of *N. magadii* L11. There was no compelling change in the intensity of the signal of the production of protein E within the samples of the wild type strain throughout the passages. *N. magadii* L11-ΔORF44 culture showed a more significant change in the ORF11 expression pattern. The expression of ORF11 was detected during the first three passages, however, after the 4th passage, the production of protein E could scarcely be observed, thus showing a behavior comparable to the cured strain *N. magadii* L13.

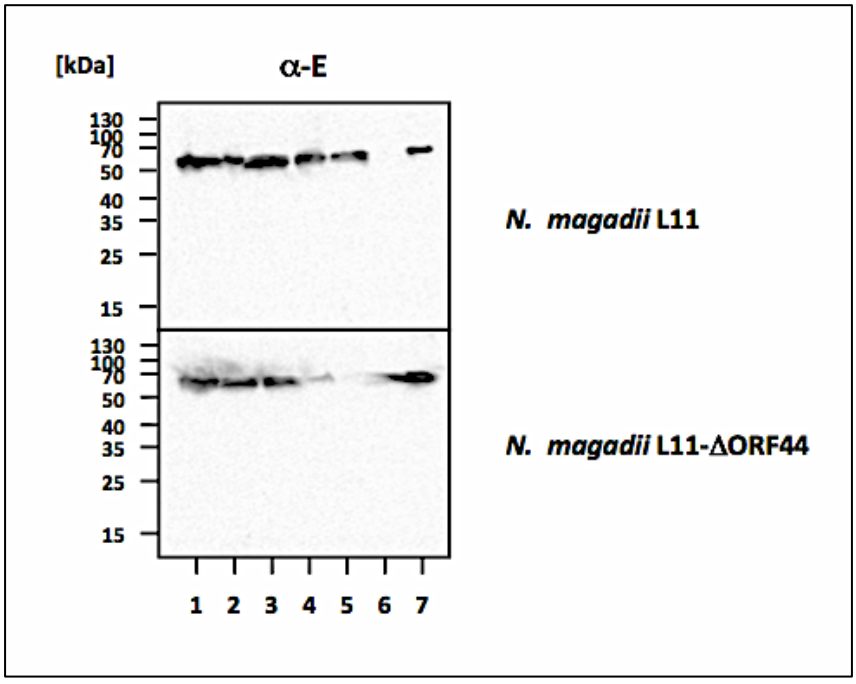

Figure 16. Expression of ORF11 in *N. magadii* L11 and *N. magadii* L11-ΔORF44.

Protein samples were prepared from *N. magadii* L11 (top panel) and *N. magadii* L11-ΔORF44 (bottom panel) that were separated on 12% SDS PAGE gel. The production of protein E was detected via Western Blot using an α-E antibody (1:2500). Lanes 1-5 represent the first five passages of the

respective cultures. Lane 7 shows isolated protein E used as a control. The expression pattern of ORF11 in the wild type did not show a significant change throughout the passages, in comparison to *N. magadii* L11-ΔORF44, wherein protein E was barely produced in the 4th passage. Furthermore, after the 5th passage, protein E was virtually absent. The size markers are indicated at the left (in kDa).

3.1.1.6. Re-infection of the presumed cured strain *N. magadii* L11-ΔORF44

As previously mentioned in the 'Introduction', re-infection of the wild type *N. magadii* L11 is not possible. However, the cured strain *N. magadii* L13 could be re-infected (Witte *et al*., 1997). As specified above, the *N. magadii* L11-ΔORF44 culture did no longer show a production of protein E after the 5th passage. This observation therefore led to the assumption that at least part of the *N. magadii* L11-ΔORF44 cells were cured from the virus through passaging the culture five times. To verify this, it was necessary to analyze if the strain *N. magadii* L11-ΔORF44 with a low virus release could be re-infected similar to the cured *N. magadii* L13. This was examined by continuously passaging the cultures until the 8th passage (see Figure 17).

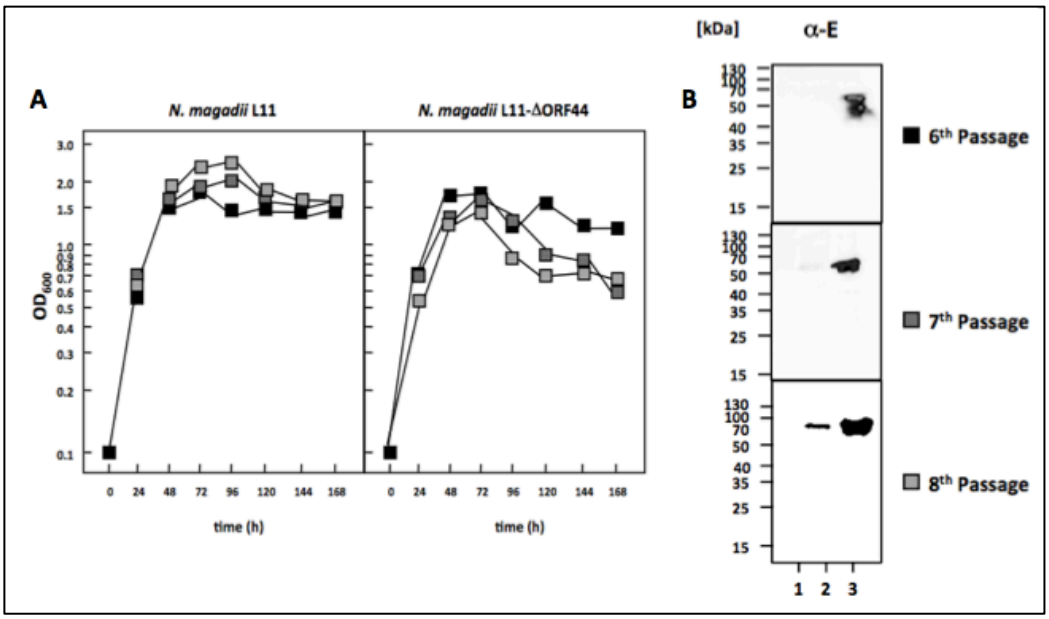

Figure 17. Growth kinetics analysis of and expression of ORF11 in the wild type *N. magadii* L11 vs. the mutant *N. magadii* L11-ΔORF44 during the 6th up to the 8th passage.

(A) Passages of cultures of the wild type *N. magadii* L11 and the mutant strain *N. magadii* L11-ΔORF44 were performed as described on section 2.2.6.1 and the optical density was measured at 600 nm. The growth kinetics of *N. magadii* L11 did no longer show an optical lysis, thus exhibiting a

similar growth behavior to the cured *N. magadii* L13. Upon re-infection of the presumed cured *N. magadii* L11-ΔORF44, stronger lysis was observable the further the culture was passaged.

(B) Western Blots of samples taken from passage 6 to 8. After separation, the proteins were transferred to a nylon membrane and incubated with an α-E-antiserum. Top panel: 6th passage, middle panel: 7th passage, bottom panel: 8th passage. Sizes of marker proteins are indicated on the left (in kDa). Lane 1 shows the expression of ORF11 in *N. magadii* L11 and Lane 2 depicts that in *N. magadii* L11-ΔORF44. In accordance to the growth kinetics analysis, *N. magadii* L11 seemed to be cured of the virus, as the culture no longer showed production of protein E from the 6th passage onwards. On the contrary, the re-infection of the supposedly cured *N. magadii* L11-ΔORF44 led to an increase of the production of protein E, thus concluding an increased viral spreading in the culture.

The wild type strain *N. magadii* L11 did not show a lysis behavior as seen before (Figure 17A). Its behavior resembles that of the cured *N. magadii* L13. This could also be observed on the Western Blot – no signals of the expression of ORF11 encoding protein E could be detected (Lane 1, Figure 17B). On the other hand, the presumed cured *N. magadii* L11-ΔORF44 was re-infected and therefore showed lysis. In accordance to the growth kinetics, the Western Blot shows an increase in the production of protein E (Lane 2, Figure 17B), thus showing an onset of lysis after the 7th passage (Figure 17A). Therefore, an increased virus particle release in the *N. magadii* L11-ΔORF44 culture was determined as evident on the virus titer assay on Figure 18. As for *N. magadii* L11, the virus titer assay shows that prolonged passage eventually results in a decrease in virus particle liberation.

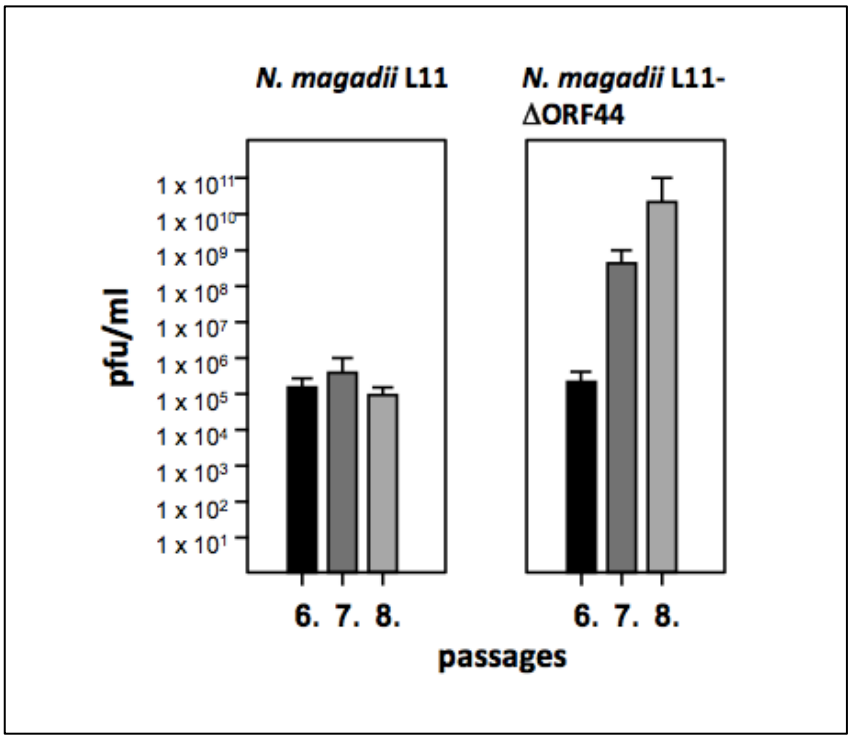

Figure 18. Virus titer analysis of *N. magadii* L11 and *N. magadii* L11- Δ ORF44.

Five days after inoculation of the cultures, samples were taken. Cells were separated from the supernatant by centrifugation. The supernatants were used to plate appropriate dilutions using top agar together with *N. magadii* L13 as an indicator strain. After 1 week of incubation at 37°C the virus titers were determined. The values of the virus titers (pfu/ml) are indicated as bars in black (6th passage), dark grey (7th passage), middle grey (8th passage). Error bars are indicated, $\pm$ 1SD.
In accordance to the growth kinetics and the Western Blot analysis, the virus titer analysis showed that upon re-infection, the presumed cured strain *N. magadii* L11- Δ ORF44 showed an increased phage particle release from the 7th to the 8th passage. As for the wild type strain *N. magadii* L11, the virus particle release decreased, in comparison to the first five passages as seen above on Figure 15.

3.1.2. Characterization of the function of gp44

Prior studies of ORF43 and ORF44, two open reading frames of the ΦCh1 genome containing overlapping start and stop codons, suggested that they are co-transcribed as well as co-translated. These observations concluded that they both form an operon together and the promoter sequences of these two ORFs could only be found upstream of ORF43 (p_{43}) (Klein *et al*., 2002).

For the two open reading frames (ORF43 and ORF44), a high similarity to the co-operative element of repressor of the virus ΦH ($Rep_{\Phi H}$) was identified within the transcripts T9/T10 (Iro *et al*., 2007). ORF43 and ORF44 overlap with their stop- and

start-codons, respectively. A ribosome-binding site could only be detected in the 5´-region of ORF43 and not of ORF44 (Klein *et al*., 2002). Putative promoter sequences were found in the 5´-regions for ORF43 as well as for ORF44. It was shown that within the lysogenic strain *N. magadii* L11, both genes (ORF43 and 44) were transcribed constitutively. Using Western Blot analysis gp44 could be detected throughout the growth of the lysogenic strain *N. magadii* L11 with an increase in ORF44 translation in the mid-logarithmic growth phase. The gene product of ORF43, gp43, does not contain any domain of known function. As a result of BgaH assays, gp43 seems to activate gene expression of the intergenic region between *rep* and ORF49 whereas gp44 reduces gene expression (Iro *et al*., 2007).

An analysis using the Pfam database with the AA sequence of the ORF44 gene product gp44, revealed a Pin domain (AA 3-126) constituting almost the entire 131 AA protein, disclosing a similarity to the type II toxin-antitoxin system VapBC (**v**irulence-**a**ssociated **p**roteins). PIN domains generally cleave single-stranded RNAs in a sequence-specific manner. Here, the putative toxin is gp44, which resembles the stable toxin VapC, and the putative antitoxin is gp43, which is comparable to the labile antitoxin VapB. Upon degradation of the antitoxin, the toxin becomes active, thus demonstrating an autoregulatory activity (Arcus *et al*., 2011).

Further observations from Hofbauer in 2015 strengthened the hypothesis of ORF43/44 being a putative TA system. The effects of both ORFs on the expression of two reporter genes ($ORF34_{52}$ encoding a tail-fibre protein and ORF94 encoding methyltransferase) were analyzed in *N. magadii* L13. The strain containing only ORF44 along with the reporter genes resulted in the production of a truncated tail-fibre protein and a 48-hour delay in the expression of ORF94. Consequently, an EMBOSS Water analysis (https://www.ebi.ac.uk/Tools/psa/emboss_water/) of the coding sequence of $ORF34_{52}$ and the upstream region of ORF94 showed a similarity score of 61.5, indicating that gp44 may have cleaved these ORFs in a sequence-specific manner.

3.1.2.1. Aim

The aim of this study was to further investigate the function of gp44, the putative toxin of the type II TA system in the native host *N. magadii*. This was done to acquire more understanding on a potential repressing and/or endoribonuclease role of gp44. Therefore, the role of the putative consensus sequence within the upstream region of the methyltransferase gene ORF94 was investigated.

3.2.1.2. Growth kinetics analysis and production of methyltransferase

Studies performed by Hofbauer in 2015 showed that the expression of ORF94 is affected by gp44, as aforementioned. The upstream sequence of ORF94 presents high similarity to the coding sequence of $ORF34_{52}$. In order to investigate, if gp44 certainly cleaves in a sequence-specific manner, a construct containing a mutated upstream region of ORF94 was created, in which an *Eco*RI site was inserted (see section 2.2.7.1.). Growth kinetics analysis was performed to compare the fully functional ORF94 and the ORF94 with the mutated upstream region (ORF94-M2) in *N. magadii* L13. As evident on Figure 19, there is only a slight difference in their growth behavior, wherein the OD_{600} of *N. magadii* L13 (pNB102-ORF94) insignificantly dropped after six days, whereas the OD_{600} of *N. magadii* L13 (pNB102-ORF94-M2) already showed a slight drop on day 3. As for the Western Blots, the production of methyltransferase in both strains did not show compelling difference. Methyltransferase was produced from day 1 after inoculation onwards.

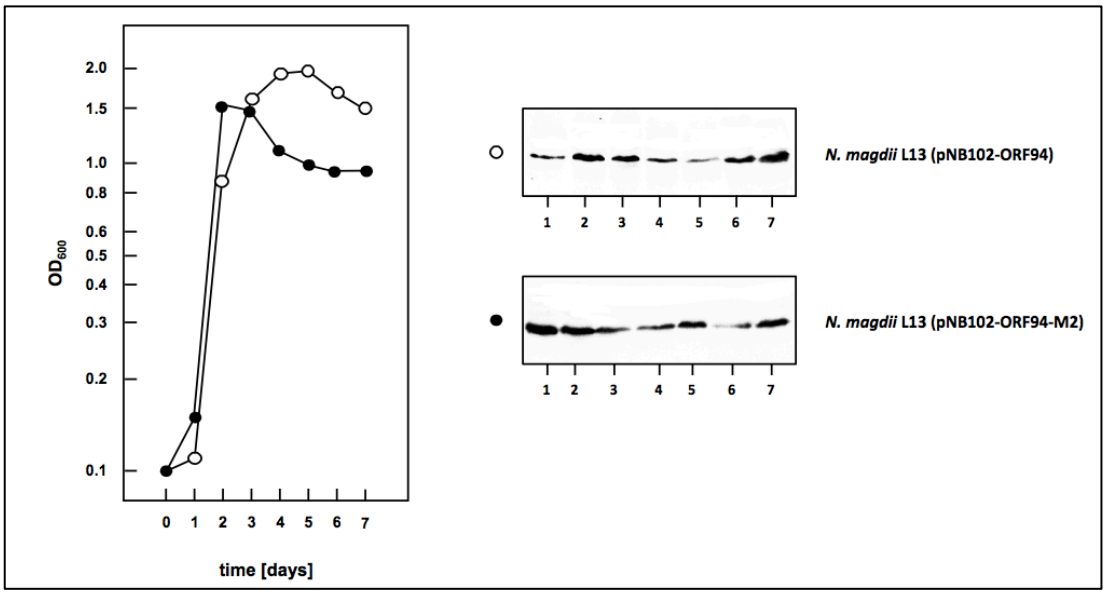

Figure 19. Growth kinetics and Western Blot analyses of the production of methyltransferase of the wild type ORF94 vs. ORF94 with the mutated upstream region (ORF94-M2) in *N. magadii* L13.

Growth kinetics of strains *N. magadii* L13 (pNB102-ORF94, open circles) and *N. magadii* L13 (pNB102-ORF94-M2, closed circles) were incubated in rich medium at 37°C with agitation. The optical density at 600 nm (OD_{600}) was measured over a time period of 7 days (left panel). Simultaneously, samples were taken and crude extracts were prepared. After separation and transfer of the proteins to a nitrocellulose membrane, Western Blots were performed with antibodies against the methyltransferase protein (right panel). The numbers below the Western Blots represent the different time points according to the growth curve given in the left panel. The different strains are indicated at the right. Sizes of marker proteins are indicated on the left (in kDa).
The growth curves depict a slight difference in their growth behavior. The optical density of the wild type ORF94 only slightly dropped on day 6, in comparison to ORF94-M2 whose OD_{600} slightly decreased on day 3. The expression of ORF94 and ORF94-M2 do not significantly differ from each other, thus both producing methyltransferase from day 1 up to day 7.

3.1.2.3. Purification of gp44 from *E. coli* under native conditions

Various attempts in purifying His-tagged gp44 (approximately 18.8 kDa: gp44= 14.7 kDa and His-tag= 4.1 kDa) under native conditions were carried out (see section 2.2.4.5.). However, after numerous attempts using different methods and elution buffers, it was still impossible to purify gp44 under native conditions due to various reasons: One of which is the fact that inclusion bodies are formed in bacterial hosts, leading to a major challenge in purifying gp44 under native conditions. Despite using the *E.coli* strain Lemo21(DE3) for transformation (see section 2.1.1.1.), which is a

suitable strain for proteins prone to insoluble expression and contains fine tuning of T7 expression that is able to alleviate inclusion body formation, gp44 was still found to be insoluble.

In addition to the protein samples prepared before and after induction, protein samples from the pellet and supernatant after harvesting the cells were also taken as well as from the resulting pellet after centrifugation of the lysed cells. These were subsequently loaded onto a 12% SDS PAGE gel to analyze where the majority of gp44 could be found. As evident on Figure 20, no gp44 could be found in the supernatant, as well as in the protein samples taken from the flow-through, the wash fractions and the eluted fractions. However, in the resulting pellet after centrifuging the lysed cells, a large amount of gp44 could be found, thus illustrating that gp44 was still insoluble.

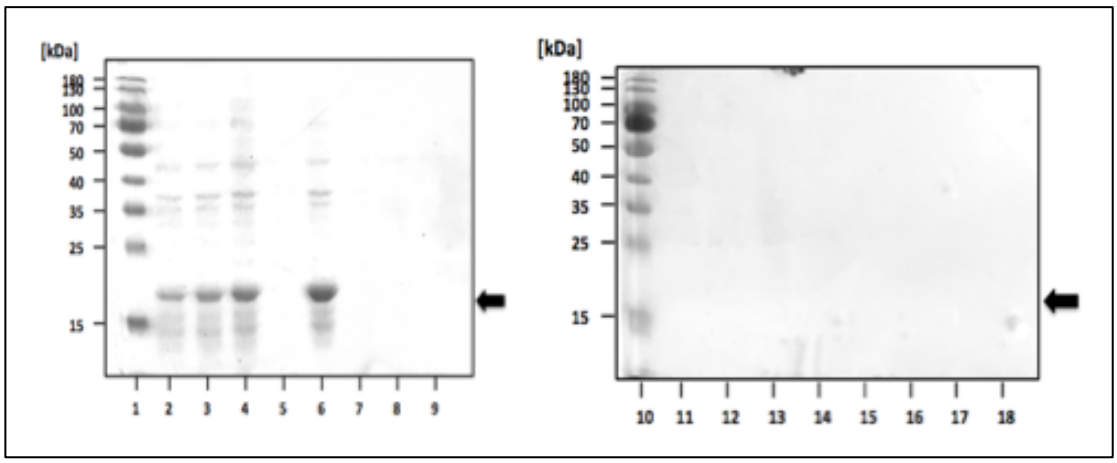

Figure 20. Purification of gp44 from Lemo21(DE3) under native conditions.

ORF44 was expressed in Lemo21(DE3) cells and the cells were lysed using sonification. The supernatant was incubated with Ni-NTA resin and the protein was eluted with raising concentrations of imidazole (2.2.4.5.). Aliquots were separated on a 12% SDS-PAGE and stained with Coomassie. The position of gp44 is indicated with an arrow on the right. Sizes of marker proteins are indicated on the left (in kDa).

Lanes 1 and 10: Prestained Protein Ladder
Lane 2: t_0 (before induction)
Lane 3: t_{240} (after 4 hours of induction)
Lane 4: Resulting pellet from the harvested cells
Lane 5: Supernatant of the harvested cells
Lane 6: Resulting pellet after the centrifugation of the lysed cells
Lane 7: Flow-through
Lane 8: Wash 1
Lane 9: Wash 2
Lanes 11-14: Elution with elution buffer (120 mM imidazole)
Lanes15-18: Elution with elution buffer (250 mM imidazole)
Elution with 500 mM imidazole is not shown, as no protein bands were visible.

The size of gp44 (indicated with an arrow) together with the His-tag is approximately 18.8 kDa. As evident on Lane 6, the majority of gp44 could be found in the resulting pellet, which indicates that gp44 was still insoluble.

3.1.2.4. Purification of gp44 from *E. coli* under denaturing conditions

Purification of gp44 from *E. coli* Lemo21(DE3) was achieved under denaturing conditions (see section 2.2.4.6.1.), due to the challenge of the previously described purification method, respectively. Gp44 was soluble and could therefore be isolated from the eluted fractions as seen on Figure 21. The fraction containing the highest concentration of gp44 was the 4th elution with Buffer D (D4).

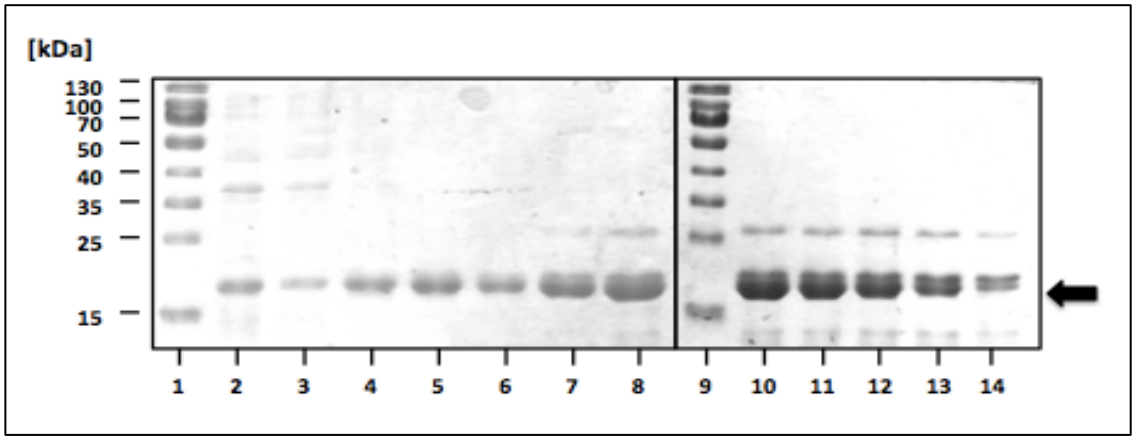

Figure 21. Purification of gp44 from Lemo21(DE3) under denaturing conditions.

ORF44 was expressed in Lemo21(DE3) cells and the cells were lysed using Buffer B. The supernatant was incubated with Ni-NTA resin and the protein was eluted with buffers of decreasing pH values (2.2.4.6.). Aliquots were separated on a 12% SDS-PAGE and stained with Coomassie. The position of gp44 is indicated with an arrow on the right. Sizes of marker proteins are indicated on the left (in kDa).

Lanes 1 and 9: Prestained Protein Ladder
Lane 2: t_{240} (4 hours after induction)
Lane 3: Flow-through
Lane 4-5: Wash 1 and 2
Lane 6-10: Elutions with Buffer D
Lane 11-14: Elutions with Buffer E

This illustrates the successful purification of gp44 (18.8 kDa) from Lemo21(DE3).

After the purification of gp44, it was necessary to renature the protein by dialysis, as it was previously purified under denaturing conditions. The purified gp44 was separately taken from the third elution with Buffer D (fraction D3) and the second

elution with Buffer E (fraction E2). As mentioned in 'Material and Methods' the purified gp44 was dialyzed against two different renaturing buffers (see on section 2.2.4.6.2.). To determine the protein concentration of the dialyzed fractions, BSA standards of certain concentrations (0.001, 0.005, 0.01, 0.05, 0.1, 0.5 µg /µl) were applied on a 12% SDS PAGE gel along with the dialyzed fractions (see Figure 22). The estimated concentration of gp44 in D3 was 0.01 µg /µl and in E2 0.03 µg /µl.

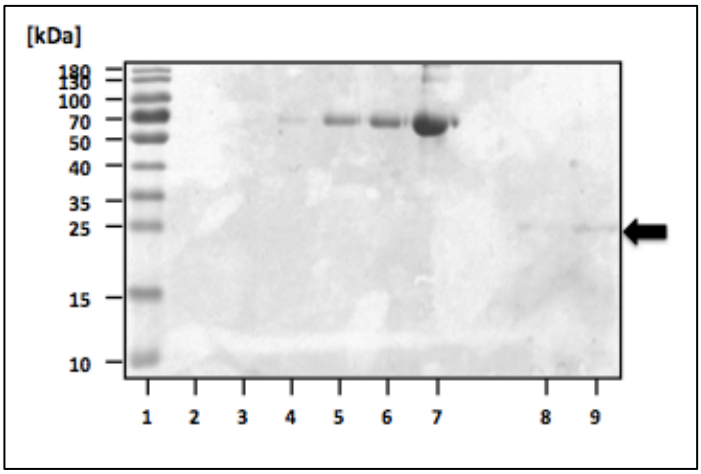

Figure 22. Quantification of gp44

Aliquots of a BSA standards as well as renatured protein gp44 were separated on a 12% SDS-PAGE and stained with Coomassie. The position of gp44 is indicated with an arrow on the right. Sizes of marker proteins are indicated on the left (in kDa).
Lane 1: Prestained Protein Ladder
Lane 2-7: BSA standards (0.001, 0.005, 0.01, 0.05, 0.1, 0.5 µg /µl)
Lane 8: 5 µl of dialyzed fraction of gp44, D3 elution
estimated concentration: 0.01 µg /µl
Lane 9: 5 µl of dialyzed fraction of gp44, E2 elution
estimated concentration: 0.03 µg /µl

The protein concentration of gp44 was determined on the basis of BSA standards of certain concentrations (0.001, 0.005, 0.01, 0.05, 0.1, 0.5 µg /µl). 5 µl of 2x Laemmli buffer was added into 5 µl of each sample, separated on a 12% SDS PAGE gel and then stained with Coomassie. The size of gp44 is approximately 18.8 kDa.

Further confirmation of the successful purification of gp44 from Lemo21(DE3) under denaturing conditions was carried out via Western Blot using α-gp44 antibody (1:500). As a control, another Western Blot was performed using α-E antibody (1:2500). Here, aliquots were again taken from the same fractions used to determine the purified gp44 concentrations: D3 and E2. Along with the protein samples from the

two fractions, isolated protein E was also loaded onto the 12% SDS PAGE gels that served as a control.

Figure 23 illustrates the successful purification of gp44, as the Western Blot with the α-gp44, signals can be observed. In accordance to the concentrations previously determined via BSA standards, gp44 from D3 had a lower concentration than that from E2, thus showing weaker signal intensity than gp44 from E2 on the Western Blot. As evident on lane 3, the control protein E could not be detected with the α-gp44 antibody, however on lane 6, the Western Blot using α-E antibody, protein E could be detected. This therefore shows that the purified proteins were specifically gp44. As for the lanes 1 and 2 where gp44 from the different fractions are located, two bands per lane could be detected: the lower bands containing approximately 30 kDa and the upper bands having about 60 kDa. The different migration of gp44 in the SDS-PAGE used for Western Blotting can be explained by the high salt concentration in the used samples (2 M NaCl).

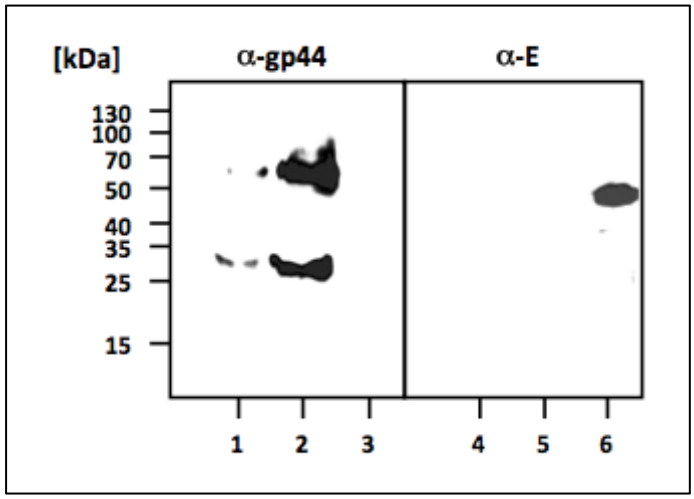

Figure 23. Western Blot analysis of the purified gp44 eluted with Buffer D and Buffer E.

Aliquots of gp44 as well as protein E were separated on a 12% SDS-PAGE and transferred to a nitrocellulose membrane. The membranes were incubated with antibodies against gp44 and protein E, respectively. Detection was performed using the Clarity™ Western ECL Substrate Kit from BioRad. The used antibodies are indicated on the top. Sizes of marker proteins are indicated on the left (in kDa).

Western Blot using α-gp44 antibody (1:500)
Lane 1: 5 µl of dialyzed fraction of gp44, D3 elution
Lane 2: 5 µl of dialyzed fraction of gp44, E2 elution
Lane 3: protein E as a control

Western Blot using α-E antibody (1:2500)
Lane 4: 5 µl of dialyzed fraction of gp44, D3 elution

Lane 5: 5 µl of dialyzed fraction of gp44, E2 elution
Lane 6: protein E as a control

The dialyzed fractions of gp44 could only be detected using the α-gp44 antibody. Lanes 1 and 2 show two bands each: the lower one having the size of 30 kDa, whereas the other band has double the size of the lower band (60 kDa).
The control protein E could only be detected using the α-E antibody.

3.1.2.5. *In vitro* transcription of ORF34 and ORF36

Further sequence analysis via EMBOSS Water sequence analysis (https://www.ebi.ac.uk/Tools/psa/emboss_water/) showed similarities in the upstream region of ORF94 with ORF34-3' and ORF36-3' (see Figure 24). These sequence similarities led to the hypothesis that gp44, the putative RNase/toxin, may also cleave ORF34-3' and ORF36-3' in a sequence-specific manner, as the similarities of these ORFs with the upstream region of ORF94 are comparable to the similarities of $ORF34_{52}$ with the upstream region of ORF94 (see Figure 11). Therefore, the constructs pRSETA-34 and pRSETA-36 were generated (see sections 2.2.7.3. and 2.2.7.4.), and then linearized with the restriction enzyme *Hind*III. Subsequently, *in vitro* transcription of the linearized pRSETA-34 and pRSETA-36 was achieved using the AmpliScribe™ T7-Flash™ Transcription Kit from Epicentre according to the manufacturer's protocol. The reaction mixtures were then incubated at 37°C for 3 hours. The successful *in vitro* transcription was then checked on 6% denaturing urea PAGE gel (see section 2.2.5.2.) (data not shown). Afterwards, the RNAs of ORF34-3' and ORF36-3' were eluted from 6% the denaturing urea PAGE gel and purified.

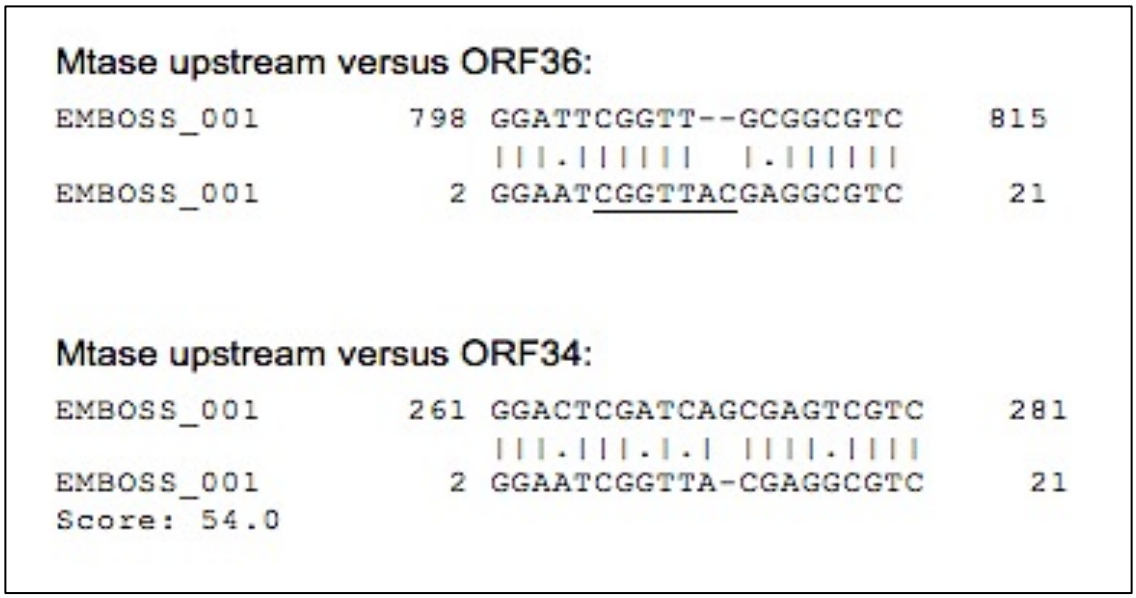

Figure 24. EMBOSS Water sequence analysis of the upstream region of ORF94 (Mtase upstream) vs. ORF36 and ORF34.

The EMBOSS Water sequence analysis (https://www.ebi.ac.uk/Tools/psa/emboss_water/) was used to align the upstream sequence of ORF94 (24 nucleotides of the untranslated region) with the coding region of ORF36 (upper panel) and the coding region of ORF34 (lower panel). The upstream sequence of ORF94 is given below the coding regions of ORF34 and ORF36, respectively. The putative consensus sequence for gp44 is underlined.
The 3' sequences of ORF34 and ORF36 were compared to the upstream region of ORF94 (Mtase upstream). This analysis also shows that the sequences show significant similarities, leading to the hypothesis that gp44 may also cleave these regions, thus cleaving in a sequence-specific manner.

3.1.2.6. mRNA interferase activity of gp44

Preliminary experiment on the mRNA interferase activity of purified gp44 was performed in this study. Purified gp44 was incubated with ORF34-3' (approximately 540 bp) and ORF36-3' (approximately 600 bp) RNAs at 37°C for 30 minutes. The reaction mixture (20 µl) consisted of each RNA, 0.03 µg gp44, 0.1 mM EDTA, 0.5 M or 2.5 M NaCl in 20 mM Tris-HCl (pH 8.0). After incubation, the products were then separated on 6% denaturing urea PAGE gels (see Figure 25). It was also important to have a control for each reaction mixture, which does not contain the gp44, to see if any differences in the RNAs arose.
It was valuable to keep in mind that due to the high salt concentrations, the migration of the samples did not run in a smooth, strain line – on the contrary, they run much slower than the RNA ladder and also migrated in a hill-shaped manner. The sizes of

the RNAs shown by the RNA ladder therefore do not correspond with the exact sizes of the particular RNAs.

As evident on Figure 25, both ORF34-3' and ORF36-3' with and without gp44, each incubated in 0.5 M and 2.5 M NaCl, contain approximately the same size. As for the band visible below the RNA ORF34-3' incubated with gp44 on lane 3 with 2.5 M NaCl, this seems to be the variation of the amount of the reaction mixture loaded onto the gel, as this band is also visible on the lanes 2 (ORF34-3' alone) and 3 (ORF34-3' with gp44) with 0.5 M NaCl. Nonetheless no other suspicious smears could be detected.

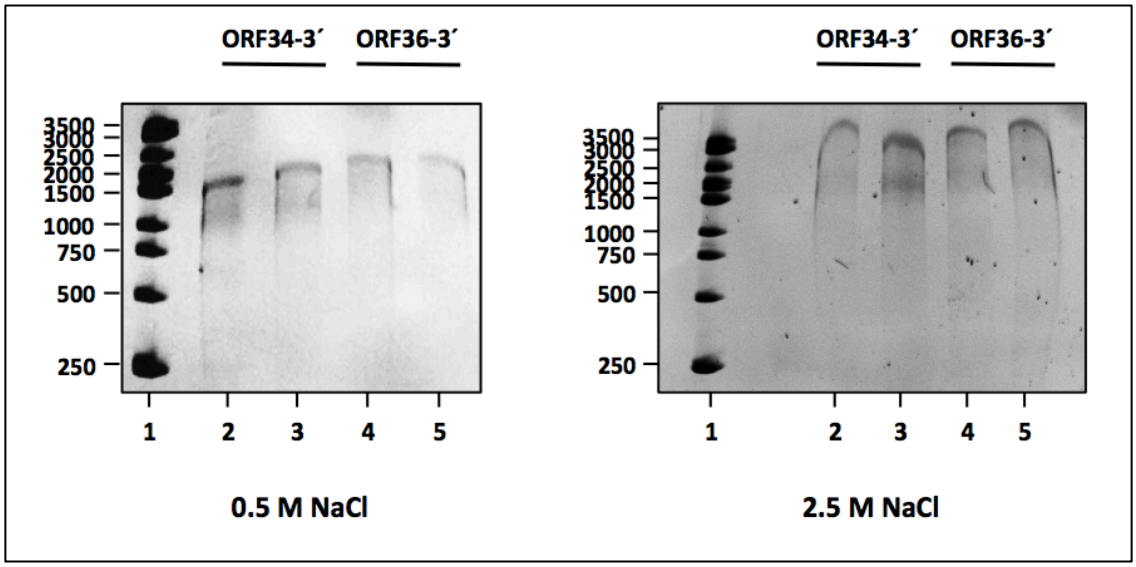

Figure 25. mRNA interferase activity of gp44 with different NaCl concentrations (0.5 M and 2.5 M NaCl).

mRNAs of the 3´-ends of ORF34 and ORF36 were produced in an *in vitro* transcription assay.

0.5 M NaCl
Lane 1: 1kb RNA Ladder
Lane 2: RNA ORF34-3' alone
Lane 3: RNA ORF34-3' incubated with gp44
Lane 4: RNA ORF36-3' alone
Lane 5: RNA ORF36-3' incubated with gp44

2.5 M NaCl
Lane 1: 1kb RNA Ladder
Lane 2: RNA ORF34-3' alone
Lane 3: RNA ORF34-3' incubated with gp44
Lane 4: RNA ORF36-3' alone
Lane 5: RNA ORF36-3' incubated with gp44

As evident on both denaturing urea PAGE gels, the RNAs of the same sequence with and without gp44 did not show any significant difference in size or appearance. The band below the RNA ORF34-3' incubated with gp44 with 2.5 M NaCl is comparable to the bands below the RNA ORF34'3 with and without gp44 on lanes 2 and 3 with 0.5 M NaCl. This indicates that the visible bands below the RNA were due to the divergence in the amount of the reaction mixture loaded onto the gels.

3.2. Discussion

The outline of this study was set to investigate the stability of the ΦCh1 ORF44 deletion mutant and to characterize the function of ΦCh1 ORF44, a 395 bp open reading frame located upstream of the ΦCh1 DNA replication module (Klein *et al*., 2002).

Iro *et al*. were the first to perform experiments with ORF43/44 in 2007, making the two ORFs good candidates in having an impact on the regulation of gene expression in ΦCh1. The results of their experiments showed that ORF43 alone and ORF43/44 have an enhancing effect on the intergenic region between ORF48 and ORF49 by conceivably binding directly or indirectly to the 5' repeats of ORF48 sequence, encoding a repressor protein *rep*, and therefore consequently enhances the transcription of ORF49, which has been reported to being involved in the activation of the lytic life cycle of ΦCh1. The reporter gene of choice for these experiments was *bga*H, whose encoded activity was examined under the control of the promoter of ORF49. The construct containing ORF44 alone resulted in lack of BgaH activity, thus suggesting that ORF44 may behave as a repressor (Iro *et al*., 2007).

Hofbauer performed preliminary experiments regarding the characterization of ΦCh1 ORF44 in *N. magadii* L13 in 2015. The effects of ORF44 on the expression of two different reporter genes were investigated: $ORF34_{52}$ encoding a tail-fibre protein and ORF94 encoding the main methyltransferase. The results of his experiments with ORF44 and the reporter genes under the control of p_{43} presented a truncated tail-fibre protein and a 48-hour delay in the production of methyltransferase, thus indicating a cleaving activity of ORF44 (Hofbauer, 2015). Furthermore, after Pfam analysis, a PIN domain in the ORF44 gene product gp44 was revealed, further suggesting that gp44 may cleave single-stranded RNA in a sequence-specific manner, just like the other known PIN domains present in the toxins of type II TA system (Arcus *et al*., 2011). To further strengthen this assumption, EMBOSS Water analysis (https://www.ebi.ac.uk/Tools/psa/emboss_water/) was performed to analyze sequence similarities within the ΦCh1 ORFs with the upstream region of ORF94, which may potentially be cleaved by gp44 in a sequence-specific manner, as it contains similar sequences with the coding sequence of $ORF34_{52}$.

Gillen executed supplementary investigations on the characterization of ΦCh1 ORF44 in 2017, wherein a ΦCh1 ORF44 deletion mutant was created in its native host *N. magadii* L11. The creation of the strain led to the experiments comparing its growth kinetics to the wild type *N. magadii* L11. His observations in regard to the spontaneous lysis of the deletion mutant and its growth behavior comparable to that of the cured strain *N. magadii* L13 after three to four passages led to the investigation of the stability of *N. magadii* L11-ΔORF44 (Gillen, 2017).

3.2.1. Stability of the ΦCh1 ORF44 deletion mutant

As aforementioned in the 'Introduction', operons consisting of toxin and antitoxin genes encode the TA systems. Toxin, among other functions, also acts as ribonuclease that degrades mRNA in either a specific or a non-specific manner. TA operons are also known to be responsible for cell survival and only the daughter cell that contains the TA genes on the plasmid, which were transferred from the parental plasmid, survive. However, when a daughter cell does not harbor the parental plasmid with the TA operon, the toxin kills the "plasmid-free" daughter cell. The toxin is released upon proteolytic degradation of the corresponding unstable antitoxin, leading to cell killing. Plasmid maintenance is thus achieved by the so-called post-segregational cell killing performed by the toxin (Gerdes *et al*., 1986). There were also reports indicating that cell killing additionally leads to reduced phage spreading (Boe *et al*., 1987).

In this study, eight total passages of an *N. magadii* L11-ΔORF44 and *N. magadii* L11 culture were performed, as to investigate the stability of the provirus ΦCh1-ΔORF44 deletion mutant upon comparison with the wild type. As evident on the results, *N. magadii* L11-ΔORF44 lysed 24 hours earlier than the wild type. This may be due to the absence of the toxin, which typically kills cells not harboring the parental plasmid containing the TA system leading to a reduced phage spreading. The lack of toxin may therefore lead to an increased virus spreading, thus causing an earlier onset of lysis on the 1st passage of the *N. magadii* L11-ΔORF44 culture.
Taking the results of the growth kinetics during the first five passages and the Western Blots together, the deletion mutant seemed to have stopped lysis comparable to the growth behavior of the cured strain *N. magadii* L13, leading to a decrease in

phage production as evident on the virus titer analysis. The *N. magadii* L11-ΔORF44 culture have stopped lysis earlier than the wild type *N. magadii* L11. Another reason for this would be the fact that since ORF44 was deleted, gp44, the putative toxin, could not be produced, thus giving rise to an excess of gp43. Considering the fact that the cells not containing the plasmids with the TA system cannot be killed, as there is no gp44, the *N. magadii* L11-ΔORF44 culture therefore stopped lysing, respectively. Further hypothesis is that, the more a culture is passaged, the more mutations arise in the genome. This may also lead to cells not lysing anymore, as the ΦCh1 genome is no longer fully functional and the virus could therefore no longer exhibit its lytic life cycle.

As already mentioned, the growth behavior of *N. magadii* L11-ΔORF44 was comparable to that of the cured *N. magadii* L13 after the 5th passage. Furthermore, it was speculated that *N. magadii* L11-ΔORF44 might have become non-lysogenic as a result of prolonged passage, thus giving rise to cells that have been cured from the virus, corresponding the cured strain *N. magadii* L13. Besides, it has been reported that *N. magadii* L11 cannot be re-infected. However, data from the growth kinetics analysis and Western Blot from the 6th up until the 8th passage showed that *N. magadii* L11-ΔORF44 was re-infected, thus showing optical lysis and production of the major capsid protein E. Re-infection in this case may have been possible due to lack of washing of the culture. The virus particles contained in the supernatants were therefore not washed away, allowing the presence of free virus particles in the culture medium and thus infecting the presumed cured *N. magadii* L11-ΔORF44. As a result, more infected cells arose, which in turn also produced viruses and therefore showed signals in the Western Blot analysis.

3.2.2. Characterization of the function of gp44

Iro *et al*. speculated in 2007 that gp44 may act as a putative repressor of the ORF49 transcription. An EMBOSS Water sequence analysis (https://www.ebi.ac.uk/Tools/psa/emboss_water/) of the upstream region of ORF94 and the reporter gene *bga*H that has been used to investigate the impact of ORF43 and/or ORF44 on the regulation of gene expression of ORF49, showed sequence

similarities with a score of 97 (see Figure 26). This therefore contradicts the assumption presented by Iro *et al*. Due to the sequence similarities of the upstream region of ORF94 and the *bga*H gene, gp44 may have cleaved the *bga*H gene instead of acting as a repressor, thus not showing any bgaH activity. This again, shows a putative cleavage in a sequence-specific fashion. This is one of the several views that have been put forward to account for the phenomenon of the sequence-specific endoribonucleolytic activity of gp44.

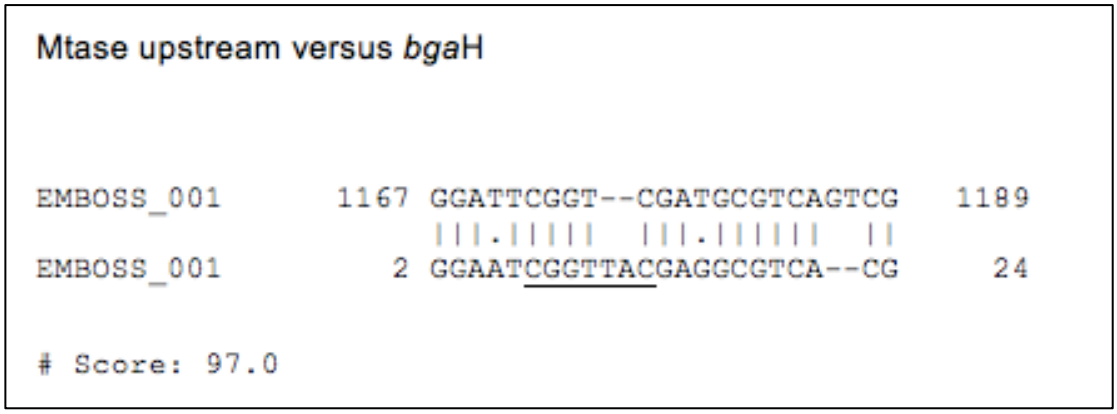

Figure 26. EMBOSS Water sequence analysis of the upstream region of ORF94 (Mtase upstream) vs. *bga*H reporter gene.

The sequence of the reporter gene *bga*H used to investigate the effect of gp44 on the transcription of ORF49 was compared to the upstream region of ORF94 (Mtase upstream). This analysis shows compelling similarities, leading to the hypothesis that gp44 may also cleave this region in a sequence-specific manner. This observation therefore contradicts the assumption made by Iro *et al*. in 2007 that gp44 may have repressed the transcription of ORF49, thus generating no BgaH activity.

Preliminary experiments on the characterization of the function of purified gp44 from *E. coli* Lemo21(DE3) was carried out during the course of this study. The Western Blot of the purified gp44 using an α-gp44 antibody shows two bands: one band containing approximately 30 kDa and the other band containing 60 kDa. The second band seems to be a dimer of gp44. It has been reported that some ribonucleases are able to form dimers near neutral pH, such as RNase A and VapC. Dimerization supposedly results in combined active sites and the ribonucleolytic activity (Park & Raines, 2000). This presumably indicates that gp44 may be active as a dimer.

The initial experiment held regarding the mRNA interferase activity of gp44 was unfortunately not conclusive, as the purified gp44 seemed not to have cleaved the

RNAs ORF34-3' and ORF36-3'. This may have happened due to various reasons: One plausible reason would be that the purified gp44 may have been inactive and therefore couldn't perform its function. Another reason would be the composition of the reaction mixture containing the RNA and the purified gp44, which in future experiments perhaps need to be more optimized. Further question emerged giving doubts to gp44 being a putative RNase: Did the purified gp44 not cleave the RNAs, because it really is not an RNase? To answer this question, more experiments with gp44 are essential. This approach may also be repeated using other RNAs, such as the RNA from the upstream region of ORF94 or the coding sequence of $ORF34_{52}$.

As for the experiments carried out with ORF94 and the mutated upstream region of ORF94 in *N. magadii* L13, no significant changes in the expression of methyltransferases have been observed. Further experiments with *N. magadii* L13-ORF94 and *N. magadii* L13-ORF94-M2 are essential to additionally confirm the ribonucleolytic activity of gp44. One of which would be the same approach Hofbauer did for his experiments with ORF44: Constructs containing ORF44 and the reporter gene ORF94 or ORF94-M2 could be transformed in *N. magadii* L13. Consequently, the expression of both reporter genes would be compared via Western Blot. Ideally, if the production of methyltransferase in the strain containing the construct with ORF94-M2 and ORF44 were similar to the production of methyltransferase in the strain without ORF44, then this would presumably give answers regarding the sequence-specific endoribonucleolytic activity of gp44 in the future.

4. References

Abedon, S. T. and Murray, K. L. 2013. "Archaeal Viruses, Not Archaeal Phages: An Archaeological Dig." *Hindawi Publishing Corporation Volume **2013**, Article ID 251245*.

Albers S. V., van de Vossenberg J. L., Driessen A. J. M. and Konings W. N. 2000. "Adaptations oft the archaeal cell membrane to heat stress." *Frontiers in Bioscience* **5**: 813-820

Albers, S. V. and Meyer, B. H. 2011. "The archaeal cell envelope." *Nature Reviews. Microbiology* **9**: 414-426.

Allers, T. 2010. "Overexpression and purification of halophilic proteins in Haloferax volcanii." *Bioengineered Bugs* **1(4)**: 288-290.

Allers, T. and Mevarech, M. 2005. "Archaeal Genetics – The Third Way". *Nature Reviews Genetics* **6(1)**: 58-73.

Arcus, V. L., McKenzie, J. L., Robson, J. and Cook, G. M. 2011. "The PIN-domain ribonucleases and the prokaryotic VapBC toxin-antitoxin array." *Protein Engineering, Design & Selection* **24(1-2)**: 33-40.

Bailey, S. E. and Hayes, F. 2009. "Influence of operator site geometry on transcriptional control by the YefM-YoeB toxin-antitoxin complex. *Journal of Bacteriology* **191**: 762-772.

Baranyi, U., Klein, R., Lubitz, W., Krüger, D. H. and Witte, A. 2000. "The archaeal halophilic virus-encoded Dam-like methyltransferase M.ΦCh1-I methylates adenine residues and complements dam mutants in the low salt environment of *Escherichia coli*." *Molecular Microbiology* **35(5)**: 1168-1179.

Barns, S. M., Delwiche, C. F., Palmer, J. D. and Pace, N. R. 1996. "Perspectives on archaeal diversity, thermophily and monophyly from environmental rRNA sequences." *Proceedings of the Natural Academy of Sciences of the United States of America* **97**: 9188-9193

Berquist, B. R. and DasSarma, S. 2003. "An Archaeal Chromosomal Autonomously Replicating Element from an Extreme Halophile, *Halobacterium* sp. Strain NRC-1." *Journal of Bacteriology*: 5959-5966.

Birkeland, N.-K., Schönheit, P., Poghosyan, L., Fiebig, A. and Klenk, H.-P. 2017. "Complete genome sequence analysis of Archaeoglobus fulgidus strain 7324 (DSM

8774), a hyperthermophilic archaeal sulfate reducer from a North Sea oil field." *Standards in Genomic Sciences* **12**: 79.

Blöchl, E., Rachel, R., Burggraf S., Hafenbradl, D., Jannasch H. W. and Stetter K. O. 1997. "*Pyrolobus fumarii*, gen. und sp. nov., represents a novel group of archaea, extending the upper temperature limit for life to 113°C." *Extremophiles* **1**: 14-21

Boe, L., Gerdes, K., Molin, S. 1987. "Effects of genes exerting growth inhibition and plasmid stability on plasmid maintenance." *Journal of Bacteriology* **169**: 4646-4650.

Brochier-Armanet, C., Forterre P. and Gribaldo, S. 2011. "Phylogeny and evolution of the Archaea: one hundred genomes later." *Current Opinion in Microbiology* **14(3)**: 274-281.

Bult, C. J., White, O., Olsen, G. J., Zhou, L., Fleischmann R. D., Sutton, G. G., Blake, J. A., FitzGerald L. M., Clayton, R. A., Gocanye, J. D., Kerlavage, A. R., Doughtery, B. A., Tomb, J. F., Adams, M. D., Reich, C. I., Overbeek, R., Kirkness, E. F., Weinstock, K. G., Merrick, J. M., Glodek, A., Scott, J. L., Geoghagen, N. S. and Venter, J. C. 1996. "Complete genome sequence of the methanogenic archaeon, *Methanococcus jannashii*." *Science* **273(5278)**: 1058-1073.

Cline, S. W. and Doolittle, W. F. 1987. "Efficient Transfection of the archaebacterium *Halobacterium halobium*." *Journal of Bacterioulogy 169(3). American Society for Microbiology*: 1341-1344.

Desiere, F., McShan, W. M., van Sinderen, D., Ferretti, J. J., and Brüssow, H. 2001. "Comparative genomics reveals close genetic relationships between phages from dairy bacteria and pathogenic streptococci: evolutionary implications for prophage-host interactions." *Virology* **288:** 325-341.

Dyall-Smith, M., Tang, S. L. and Bath, C. 2003. "Haloarchaeal viruses: How diverse are they?" *Research in Microbiology* **154**: 309-313.

Fendrihan, S., Legat, A., Pfaffenhuemer, M., Gruber, C., Weidler, G., Gerbl, F. and Stan-Lotter, H. 2006. "Extremely halophilic *Archaea* and the issue of long-term microbial survival." *Reviews in Environmental Science and Biotechnology (Online)* **5(2-3)**: 203-218

Forterre, P., Brochier, C. and Philippe, H. 2002. "Evolution of the *Archaea*." *Theoretical Population Biology* **61(4)**: 409-422.

Gerdes, K., Rasmusse, P. B. and Molin, S. 1986. "Unique type of plasmid maintenance function: Postsegregational killing of plasmid-free cells." *Proceedings of the National Academy of Sciences of the United States of America* **83**: 3116-3120

Gillen, Y. 2017. "Construction of mutant ΦCh1-ΔORF44, its characterization and first steps in the generation of mutant ΦCh1-ΔORF56." *Master thesis*.

Grant, W. D., Gemmell, R. T. and McGenity, T. J. 1998. "*Halobacteria*: the evidence for longevity." *Extremophiles* **2(3)**: 279-87.

Gribaldo, S. and Brochier-Armanet, C. 2006. "The origin and evolution of *Archaea*: a state of the art." *Philosophical Transactions of the Royal Society B* **361**:1007-1022.

Haeckel, E. 1866. "Generelle Morphologie der Organismen. Allgemeine Grundzüge der organischen Formen-Wissenschaft, mechanisch begründet durch die von Charles Darwin reformierte Descendenztheorie." *Berlin, G. Reimer*.

Hofbauer, C. 2015. "The function of gp34 and its regulation by ORF79 of ΦCh1 as well as the influence of other regulation elements. *Master thesis*.

Hogg, S. "Essential Microbiology." West Sussex: *John Wiley & Sons Ltd*, 2005. Print.

Holcik, M. and Iyer, V. N. 1997. "Conditionally lethal genes associated with bacterial plasmids." *Microbiology* **143(Pt11)**: 3403-3416.

Holmes, M. L. and Dyall-Smith, M. L. 1991. "Mutations in DNA gyrase result in novobiocin resistance in halophilic archaebacteria." *Journal of Bacteriology* **173(2)**: 642-648.

Huber, H., Hohn, M. J., Rachel, R., Fuchs, T., Wimmer, V. C. and Stetter, K. O. 2002. "A new phylum of *Archaea* represented by a nanosized hyperthermophilic symbiont." *Nature* **417(6884)**: 63-67.

Iro, M. 2006. "Characterization of the regulatory region of the virus ϕCh1 infecting *Natrialba magadii*". *Dissertation*.

Iro, M., Klein, R., Gálos, B., Baranyi, U., Rössler, N. and Witte, A. 2007. "The lysogenic region of virus ΦCh1: identification of a repressor-operator system and determination of its activity in halophilic *Archaea*." Extremophiles **11**: 383-396

Jarrell K. F., Walter A. D., Bochiwal C., Borgia J. M., Dickinson, T. and Chong, J. P. J. 2011. "Major players on the microbial stage: why archaea are important." *Microbiology* **157**: 919-936

Kamekura, M., Dyall-Smith, M. L., Upasani, A., Ventosa, A. and Kates, M. 1997. "Diversity of alkaliphilic halobacteria: Proposals for transfer of *Nanobacterium vacuolatum, Natronobacterium magadii,* and *Natronobacterium pharaonis* to *Halorubrum*, *Natrialba*, and *Natronomonas* gen. nov., respectively, as *Halorubrum vacuolatum* comb. nov*., Natrialba magadii* comb. nov., and *Natronomonas pharaonis* comb. nov., respectively." *International Journal of Systematic Bacteriology* **47(3)**: 853-857

Kates, M. "The Biochemistry of *Archaea* (*Archaebacteria*)." Amsterdam: *Elsevier*, 1993. Print.

Kennedy, S. P., Ng, W. V., Salzberg, S. L, Hood, L. and DasSarma, S. 2001. "Understanding the adaptation of *Halobacterium* species NRC-1 to its extreme environment through computational analysis of its genome sequence." *Genome Research* **11**: 1641-1650

Klein, R., Baranyi, U., Rössler, N., Greineder, B., Scholz, H. and Witte, A. 2002. "*Natrialba magadii* virus ΦCh1: first complete nucleotide sequence and functional organization of a virus infecting a haloalkaliphilic archaeon." *Molecular Microbiology* **45(3)**: 851-863.

Klingl, A. 2014. "S-layer and cytoplasmic membrane – exceptions from the typical archaeal cell wall with a focus on double membranes." *Frontiers in Microbiology. Microbial Physiology and Metabolism* **5(624)**: 1-6.

König, H., Rachel, R. and Claus, H. "Proteinaceous surface layers of archaea: ultrastructure and biochemistry." Washington, DC: *American Society of Microbiology Press, in Archaea: Molecular and Cell Biology, ed. R. Cavicchioli*. 315-340. 2007. Print.

Kushner, D. J. and Kamekura, M. "Physiology of halophilic eubacteria." Boca Raton, Florida: *CRC Press. Halophilic Bacteria 1* (Rodriguez-Valera F. ed) p. 109-138. 1988. Print.

Lanyi, J. K. 1974. "Salt-dependent properties of proteins from extremely halophilic *Bacteria*." *American Society for Microbiology. Bacteriological Reviews* **38(3)**:272-290.

Lawrence, J. G., Hendrix, R. W. and Casjens, S. 2001. "Where are the pseudogenes in bacterial genomes?" *Trends Microbiol* **9:** 535–540.

Lewis, K. 2010. “Persister cells.” *Annual Review of Micriobiology* **64**: 357-372.

Linnaeus, C. 1735. “Systema naturae, sive Regna tria naturae. Systematice proposita per Classes, Ordines, Genera, & Species.” *Lugduni Batavorum, Apud Theodorum Haak.*

Marcotte, E. M., Pellegrini, M., Thompson, M. J., Yeates, T. O. and Eisenberg, D. 1999. “A combined algorithm for genome-wide prediction of protein function.” *Nature* **402**: 83-86.

Mayrhofer-Iro, M., Ladurner, A., Meissner, C., Derntl, C., Reiter, M., Haider, F., Dimmel, K., Rössler, N., Klein, R., Baranyi, U., Scholz, H. and Witte, A. 2013. “Utilization of virus ΦCh1 elements to establish a shuttle vector system for halo(alkali)philic *Archaea* via transformation of *Natrialba magadii*.” *Applied and Environmental Microbiology* **79(8)**: 2741.

Mutschler, H., Gebhardt, M., Shoeman, R. L. and Meinhart, A. 2011. “A novel mechanism of programmed cell death in bacteria by toxin-antitoxin systems corrupts peptidoglycan synthesis. *PLoS Biology* **9**: e1001033.

Oren, A. 1999. “Bioenergetic aspects of halophilism.” *Microbiology and Molecular Biology Reviews* **63**: 334-348

Oren, A. 2002. “Molecular ecology of extremely halophilic *Archaea* and *Bacteria*.” *Federation of European Microbiological Societies. Microbiology Ecology* **39**:1-7.

Pandey, D. P. and Gerdes, K. 2005. “Toxin-antitoxin loci are highly abundant in free-living but lost from host-associated prokaryotes.” *Nucleic Acids Research* **33**: 966-976

Park, C. and Raines, R. 2000. “Dimer formation by a “monomeric” protein.” *Protein Science* **9**: 2026-2033.

Pikuta, E. V. 2011. “Overview of *Archaea*.” *Proc. SPIE 8152, Instruments, Methods, and Missions for Astrobiology XIV*. 81520N.

Prangishvili, D. 2006. “Hyperthermophilic virus-host systems: detection and isolation.” *Methods in Micriobiology* **35**: 331-347.

Reed, C. J., Lewis, H., Trejo, E., Winston, V. and Evilia, C. 2013. “Protein adaptations in archaeal extremophiles.” *Archaea* **2013**: 373275.

Roberts, M. F. "Organic compatible solutes of halotolerant and halophilic microorganisms." *Saline Systems* **1**: 5.

Rotschild, L. J. and Mancinelli, R. L. 2001. "Life in extreme environments." *Nature* **409**: 1092-1101.

Sapp, J. 2005. "The prokaryote-eukaryote dichotomy: meanings and mythology." *Microbiol. Mol. Biol. Rev.* **69(2)**: 292-305.

Sarmiento, F., Long, F., Cann, I. and Whitman, W. B. 2014. "Diversity of the DNA replication system in the *Archaea* domain." *Hindawi Publishing Corporation. Archaea Volume **2014**, Article ID 675946.*

Schleper, C., Jurgens, G. and Jonusheit, M. 2005. "Genomic studies of uncultivated *Archaea*." *Nature Reviews. Microbiology* **3**: 479-488

Schnabel, H. and Zillig, W. 1984. "Circular structure of the genome of phage ΦH in a lysogenic *Halobacterium halobium.*" *Molecular and General Genetics* **193(3)**: 422-426.

Shahmohammadi, H. R., Asgarani E., Terato, H., Saito, T., Ohyama, Y., Gekko K., Yamamoto, O. and Ide, H. 1998. "Protective roles of bacterioruberin and intracellular KCl in the resistance of *Halobacterium salinarum* against DNA-damaging agents." *Journal of Radiation Research* **39(4)**: 251-262.

Siddaramappa, S., Challacombe, J. F., DeCastro, R. E., Pfeiffer, F., Sastre, D. E., Giménez, M. I., Paggi, R. A., Detter, J. C., Davenport, K. W., Goodwin, L. A., Kyrpides, N., Tapia, R., Pitluck, S., Lucas, S., Woyke, T. and Maupin-Furlow, J. A. 2012. "A comparative genomics perspective on the genetic content of the alkaliphilic haloarchaeon *Natrialba magadii* ATCC 43099^{T}." *BioMed Central Genomic* **13**: 165

Sorek, R., Kunin, V. and Hugenholtz, P. 2008. "CRISPR—a widespread system that provides acquired resistance against phages in bacteria and archaea." *Nature Reviews Microbiology* **6(3)**: 181-186.

Tadeo, X., López-Méndez, B., Trigueros, T., Laín, A., Castaño, D. and Millet, O. 2009. "Structural basis for the aminoacid composition of proteins from halophilic *Archaea*." *PLOS Biology* **7**.

Tindall, B. J., Ross, H. N. M. and Grant, W. D. 1984. "*Nanobacterium* gen. nov. and *Natronococcus* gen. nov., two New genera of haloalkaliphilic archaebacteria." *Systematic and Applied Microbiology* **5(1)**: 41-47.

Torsvik, T. and Dundas I. D. 1974. "Bacteriophage of *Halobacterium salinarium*." *Nature* **248(450)**: 680-681.

Van de Vossenberg, J. L., Driessen, A. J., Grant, W. D. and Konings, W. N. 1999. "Lipid membranes from halophilic and alkali-halophilic *Archaea* have a low H^+ and Na^+ permeability at high salt concentration." *Extremophiles*: 253-257.

Van Melderen, L. 2010. "Toxin-antitoxin systems: why so many, what for?" *Current Opinion in Microbiology* **13**: 781-785.

Van Melderen, L. and Saavedra De Bast, M. 2009. "Bacterial toxin-antitoxin systems: more than selfish entities?" *PLOS Genetics* **5**: 1-6.

Ventura, M., Canchaya, C., Kleerebezem, M., de Vos, W. M., Siezen, R. J., and Brüssow, H. 2003. "The prophage sequences of *Lactobacillus plantarum* strain WCFS1." *Virology* **316:** 245-255.

Wais, A. C., Kon, M., MacDonald R. E. and Stollar, B. D. 1975. "Salt-dependent bacteriophage infecting *Halobacterium cutirubrum* and *H. halobium*." *Nature* **256(5515)**: 314-315.

Whittaker, R. 1969. "New concepts of kingdoms or organisms. Evolutionary relations are better represented by new classifications than by the traditional two kingdoms." *Science*. **163**: 150-194.

Witte, A., Baranyi, U., Klein, R., Sulzner, M., Luo, C., Wanner, G., Krüger, D. H. and Lubitz, W. 1997. "Characterization of *Natronobacterium magadii* phage phi Ch1, a unique archaeal phage containing DNA and RNA." *Molecular Microbiology* **23(3)**: 603-616

Woese, C. R. and Fox, G. E. 1977. "Phylogenetic structure of the prokaryotic domain: the primary kingdoms." *Proceedings of the National Academy of Sciences of the United States of America* **74(11)**: 5088-5090.

Woese, C. R., Kandler, O. and Wheelis, M. 1990. "Towards a natural system of organisms: proposal for the domains *Archaea*, *Bacteria*, and *Eucarya*." *Proceedings of the Natural Academy of Sciences of the United States of America* **87(12)**: 4576-4579.

Yamaguchi, Y. and Inouyi, M. 2009. "mRNA interferases, sequence-specific endoribonucleases from the toxin-antitoxin systems." *Progress in Molecular Biology and Translational Science* **85**: 467-500

Yamaguchi, Y., Park, J-H. and Inouye, M. 2011. "Toxin-Antitoxin Systems in *Bacteria* and *Archaea*." 2011. *Annual Reviews of Genetics* **45**: 61-79

Yurist-Doutsch, S., Chaban, B., VanDyke, D. J., Jarrell, K. F. and Eichler, J. 2009. "Sweet to the extreme: protein glycosylation in archaea." *Molecular Micriobiology* **68**: 1079-1084.

Zhou, M., Xiang, H., Sun, C. and Tan, H. 2004. "Construction of a novel shuttle vector based on an RCR-plasmid from a haloalkaliphilic archaeon and transformation into other haloarchaea." *Biotechnology Letters* **26:** 1107-1113.

5. Abstract

Investigation of the transcriptional regulation of the virus ΦCh1 infecting the haloalkaliphilic archaeon *Natrialba magadii* is essential to further comprehend the regulation of its temperate life cycle. In order to gain more understanding concerning the viral transcriptional regulation, further characterization of the previously investigated ΦCh1 open reading frame 44 (ORF44), encoding a putative toxin (gp44), is necessary. The stable toxins typically build toxin-antitoxin (TA) operons together with their cognate labile antitoxins. ORF43 and ORF44 have overlapping start and stop codons, indicating that both genes are co-transcribed and co-translated. Preliminary experiments performed with ORF44 suggested that it potentially confers a repressing and/or an endoribonucleolytic function. Pfam analysis revealed a PIN domain in gp44, which generally cleaves single-stranded RNA in a sequence specific manner, thus potentially making gp44 the VapC of a VapBC TA system (type II TA system).

The first part of this thesis discusses the stability of the ΦCh1 ORF44 deletion mutant, wherein the wild type *N. magadii* L11 and the *N. magadii* L11-ΔORF44 cultures were passaged. The growth kinetics of both strains were analyzed, Western Blot analyses and virus titer assays were performed, demonstrating the growth behaviors as well as the production of progeny viruses in these strains after onset of lysis during the course of the passages. The results gathered from these experiments show that ORF44 seems to influence the stability of ΦCh1 in the lysogenic phase. *N. magadii* L11-ΔORF44 may have become non-lysogenic as a result of prolonged passage, thus generating cells that have potentially been cured from the virus comparable to the cured strain *N. magadii* L13.

The second part of this thesis deals with the initial trials to identify the function of the putative toxin gp44. The assumption that gp44 may be a putative repressor was contradicted after an “EMBOSS Water Pairwise Sequence Alignment” analysis of the utilized reporter gene bgaH, which showed significant similarities in the sequence of the gene potentially targeted by the putative endonuclease gp44. The putative toxin gp44 was purified and Western Blot analysis showed a dimerization of gp44, leading

to the assumption that gp44 may be active as a dimer, in accordance to the reports regarding dimerization of other endonucleases. The initial experiment held to investigate the mRNA interferase activity of gp44, however, did not lead to conclusive results, as the purified gp44 seemed not to have cleaved the RNAs used for this analysis. This may have happened due to the fact that the purified gp44 may have been inactive and/or the *in vitro* procedure of the RNA incubated with gp44 still needed to be optimized. Further investigations in the future should therefore be made to successfully characterize the function of gp44.

6. Zusammenfassung

Die Erforschung der transkriptionellen Regulation des Virus ΦCh1, welches das haloalkaliphile Archaeon *Natrialba magadii* infiziert, ist essentiell, um die Regulation dessen temperenten Lebenszyklus weiterführend zu verstehen. Um mehr Verständnis bezüglich der viralen transkriptionellen Regulation zu erhalten, ist eine weitere Charakterisierung des bislang erforschten ΦCh1 offenen Leserahmen 44 (ORF44), der ein vermeintliches Toxin (gp44) kodiert, wichtig. Die stabilen Toxine bilden normalerweise zusammen mit deren entsprechenden labilen Antitoxine Toxin-Antitoxin (TA) Operone. ORF43 und ORF44 enthalten überlappende Start- und Stoppcodons, welche darauf hinweisen, dass beide Gene co-transkribiert und co-tranlatiert werden. Einleitende ausgeführte Experimente mit ORF44 schlagen vor, dass er potentiell eine Repressor- und/oder eine Nukleasefunktion ausübt. Eine Pfam-Analyse zeigte eine PIN-Domäne in gp44, welche generell einzelsträngige RNA in einer sequenz-spezifischen Weise schneidet, und dementsprechend wird gp44 potentiell zum VapC eines VapBC TA-Systems (Typ II TA-System).

Der erste Teil dieser Masterarbeit beschäftigt sich mit der Stabilität der ΦCh1 ORF44 Deletionsmutante. Dazu wurden die Kulturen des Wildtyps *N. magadii* L11 und des *N. magadii* L11-ΔORF44 passagiert. Die Wachstumskinetik beider Stämme wurde analysiert, Western Blot Analysen und Virustiterassays wurden durchgeführt, die das

Wachstumsverhalten sowie die Produktion der Virusnachkommen in diesen Stämmen nach Beginn der Lyse im Laufe der Passagen zeigten. Die Ergebnisse dieser Experimente zeigen, dass ORF44 die Stabilität des ΦCh1 in der lysogenen Phase zu beeinflüssen scheint. *N. magadii* L11-ΔORF44 zeigte einen Verlust der Lyse und eine Reduzierung der Virusfreisetzung. Folglich wurden Zellen generiert, die möglicherweise von dem Virus geheilt wurden, so wie der geheilte Stamm *N. magadii* L13.

Der zweite Teil dieser Arbeit beschreibt die ersten Versuche, um die Funktion des vermeintlichen Toxins gp44 zu identifizieren. Die Annahme, dass gp44 ein vermeintliches Repressor ist, wurde nach einer „EMBOSS Water Pairwise Sequence Alignment" Analyse des verwendeten *bga*H Reportergen widersprochen, da es signifikante Sequenzähnlichkeiten mit den Genen, die möglicherweise durch die vermeintliche Endonuklease gp44 geschnitten werden, zeigt. Das vermeintliche Toxin gp44 wurde gereinigt und eine Western Blot Analyse zeigte eine Dimerisierung des gp44, welche zu einer Vermutung führt, dass gp44 als ein Dimer aktiv ist. Dies würde mit anderen Untersuchungen hinsichtlich Dimerisierung anderer Endonukleasen übereinstimmen. Das anfängliche Experiment, das zur Untersuchung der mRNA-Interferase Aktivität von gp44 durchgeführt wurde, führte jedoch nicht zu schlüssigen Ergebnissen, da das gereinigte gp44 die RNAs, die für diese Analyse verwendet wurden, nicht gespalten zu haben schien. Der Grund dafür könnte die Tatsache gewesen sein, dass das gereinigte gp44 möglicherweise inaktiv war und/oder das *in vitro* Verfahren der RNA, die mit gp44 inkubiert wurde, noch optimiert werden müsste. Weitere Erforschungen in der Zukunft sollten deswegen durchgeführt werden, um die Funktion der gp44 erfolgreich zu charakterisieren.